Article

Discovery of Quinazolin-4(3H)-ones as NLRP3 Inflammasome Inhibitors: Computational Design, Metal-free Synthesis and In-vitro Biological Evaluation

Mohd Abdullaha, Shabber Mohammed, Mehboob Ali, Ajay Kumar, Ram A. Vishwakarma, and Sandip B. Bharate

J. Org. Chem., **Just Accepted Manuscript** • Publication Date (Web): 21 Mar 2019

Discovery of Quinazolin-4(*3H*)-ones as NLRP3 Inflammasome Inhibitors: Computational Design, Metal-free Synthesis and In-vitro Biological Evaluation

Mohd Abdullaha,[†‡] Shabber Mohammed,[†‡] Mehboob Ali,[‡ǁ] Ajay Kumar,[‡ǁ]

Ram A. Vishwakarma,[†‡] Sandip B. Bharate[†‡]*

[†]Medicinal Chemistry Division, CSIR-Indian Institute of Integrative Medicine, Canal Road, Jammu-180001, India

[‡]Academy of Scientific & Innovative Research, CSIR-Indian Institute of Integrative Medicine, Canal Road, Jammu-180001, India

[ǁ]PKPD Toxicology & Formulation Division, CSIR - Indian Institute of Integrative Medicine, Canal Road, Jammu-180001, India

TOC

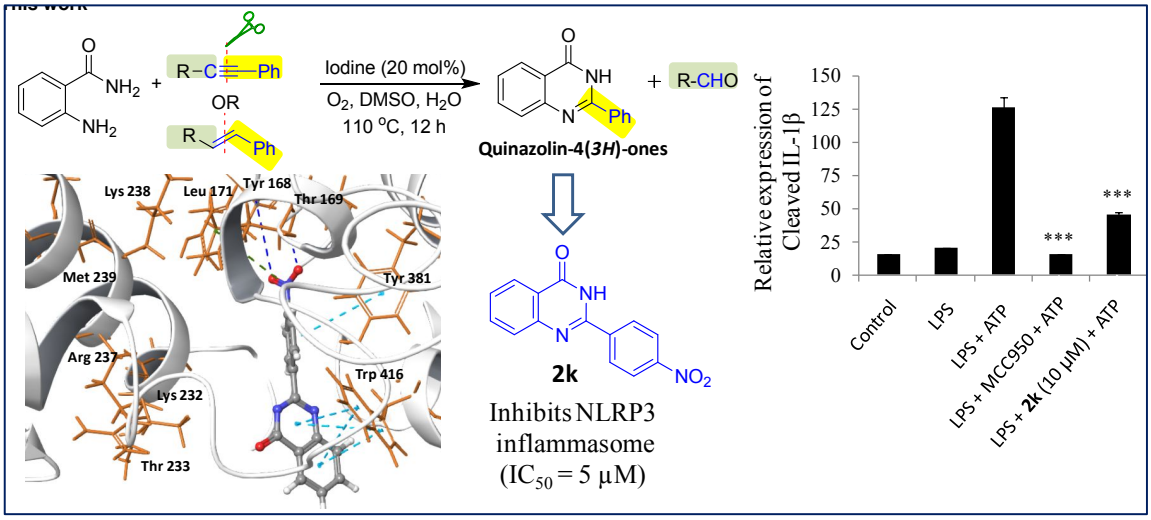

ABSTRACT.

NLRP3 inflammasome is an important therapeutic target for number of human diseases. Herein, a computationally-designed series of quinazolin-4(*3H*)-ones were synthesized using iodine-catalyzed coupling of arylalkynes (or styrenes) with *O*-aminobenzamides. Key event in this transformation involves oxidative-cleavage of C–C triple bond and the release of formaldehyde. Reaction relies on the C-N bond formation along with C-C bond cleavage under metal-free conditions. The nitro-substituted quinazolin-4(*3H*)-one **2k** inhibited NLRP3-inflammasome (IC_{50} 5 μM) *via* suppression of IL-1β release from ATP-stimulated J774A.1 cells.

KEYWORDS.

NLRP3-inflammasome; Homology model; quinazolin-4(*3H*)-ones; C-C triple bond; aminobenzamides; alkynes; Alzheimer's disease.

INTRODUCTION

The NLRP3 inflammasome play an important role in the pathogenesis of wide range of human diseases including Alzheimer's disease,[1] diabetic encephalopathy,[2] rheumatoid arthritis,[3] chronic liver disease,[4] gout,[5] cryopyrin-associated periodic syndrome (CAPS), etc.[6] The NLRP3 protein belongs to the family of nucleotide-binding and oligomerization domain-like receptors (NLRs). In addition to the NLRP3 protein, the NLRP3 inflammasome also contains adapter protein apoptosis-associated speck-like protein (ASC) and procaspase-1. The interaction between these three proteins tightly regulates the inflammasome function in order to ensure immune activity.[7] The active caspase-1 released from NLRP3 inflammasome converts pro-IL-1β to its mature form IL-1β, which is a potent pro-inflammatory cytokine involved in the process of inflammation.

In recent years, number of small molecules have been identified as inhibitors of NLRP3 inflammasome.[8] The inhibition of this complex has been achieved by small molecules, *via* inhibiting ATP-sensitive potassium channels (e.g. glyburide),[9] inhibiting the activation of caspase-1 (e.g. parthenolide),[10] inhibiting NLRP3 ATPase activity (e.g. parthenolide, Bay 11-7082,[10] acrylamide derivative[11]), inhibiting the release of IL-1β (e.g. MCC950[12]) and *via* inhibition of ATP receptor P2X7 (e.g. AZD9056) (Figure 1).[13] The β-estradiol[14] has been reported to inhibit levels of IL-1β, caspase-1 as well as P2X7 receptor.[14] OLT1177, 3-(methylsulfonyl)propanenitrile, inhibits the IL-1β release as well as caspase-1 activity, and has been advanced to the clinical trials in patients with knee osteoarthritis. Majority of the reported NLRP3 inflammasome inhibitors are sulphonyl derivatives and thus identification of new chemotype (non-sulphonyl) would be an important addition to NLRP3 inhibitors. The structure-based drug design approach provides an opportunity to come up with the new chemotype; therefore herein we employed computational approach to design quinazolin-4(*3H*)-ones as a new class of NLRP3 inflammasome inhibitors.

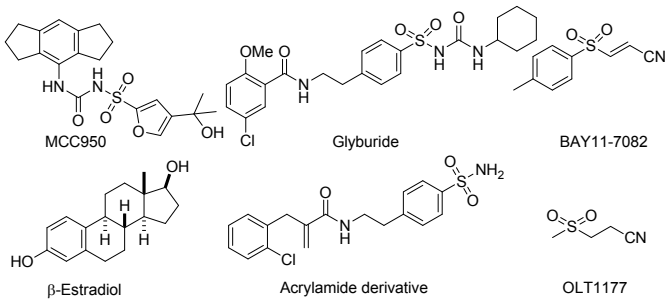

Figure 1. Structures of representative NLRP3 inflammasome inhibitors

Because of the biological importance of quinazolin-4(*3H*)-ones,[15] it has been explored extensively by synthetic chemists.[16] The condensation of *O*-aminobenzamides with aldehydes in the presence of oxidants such as $CuCl_2$,[17] DDQ,[18] MnO_2,[19] and $KMnO_4$[20] is one of the most elegant approach for its synthesis. In recent years, numerous protocols involving sp^3 carbon synthons such as benzyl halides,[21] benzyl alcohols,[22] and benzyl amines[23] have been reported. Pd catalyzed condensation with aryl halides *via* carbon insertion from CO[24] or isocyanide[25] are also reported. Other reported coupling partners include aryl carboxylic acid,[26] aryl acid chloride,[27] methylarenes.[28] Cheng and Cui's group[29] reported TFA mediated synthesis of 2-arylquinazolin-4(*3H*)-ones *via* condensation of *O*-aminobenzamides with ketoalkynes. This transformation involved TFA mediated C-C triple bond cleavage of ketoalkynes producing 2-arylquinazolin-4(*3H*)-ones along with acetophenone as a byproduct. However, to the best of our knowledge, the synthesis of 2-arylquinazolin-4(*3H*)-ones directly from terminal alkynes and styrenes has never been reported. Furthermore, the use of terminal alkynes / styrenes has several advantages over ketoalkynes, in terms of cost and commercial availability. In continuation to our interest in synthesis of medicinally important heterocycles,[30] and to validate computationally designed new NLRP3 inflammasome inhibitors, herein we have synthesized a series of 2-arylquinazolin-

4(*3H*)-ones *via* coupling of *O*-aminobenzamides with terminal aryl alkynes (and also with styrenes) under metal-free condition using molecular oxygen as an oxidant (Figure 2).

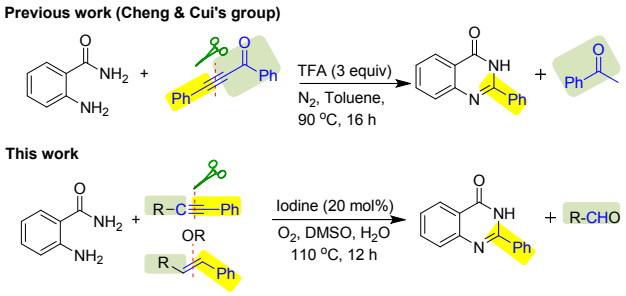

Figure 2. Synthesis of quinazolin-4(*3H*)-ones *via* coupling of *O*-aminobenzamide with aryl alkynes/ styrenes

The homology model based design followed by synthesis and biological evaluation for suppression of IL-1β release has resulted in identification of quinazolin-4(*3H*)-one as a new class of NLRP3 inflammasome inhibitors. The computational design, new synthetic strategy and biological evaluation of the series of quinazolin-4(*3H*)-ones is presented in this paper.

RESULTS AND DISCUSSION

Building Homology Model and Design of NLRP3 Inflammasome Inhibitors. The lack of crystal structure of any molecular target always adds challenges to medicinal chemists to design new class of modulators. Here, we performed the protein structure alignment of NACHT domain of the human NLRP3 protein (residues 220–536, Entry Id: Q96P20, Entry Name: NLRP3_HUMAN) with the resolved structure of NLRC4 (PDB ID: 4KXF).[31] The homology model was developed by multiple-thread alignments, as described by Zhang's research group through a web server (I-TASSER).[32] The prepared model was validated by studying the interaction of ATP and a known NLRP3 inflammasome inhibitor, MCC950. The ATP binding

site of the built protein contains a highly conserved residue Lys 232. The docking studies were performed by preparing a grid around this residue. The docking of ATP at this site has shown that its phosphate groups display several key H-bonding interactions with Lys 232, Arg 237, Thr 233 and His 522 residues. In addition, the Arg 237 residue have shown H-bonding with ATP sugar moiety and Trp 416 residue display π-π stacking with adenine base (Figure 3B).

The structure of β-estradiol could be mimicked *via* 2-aryl quinazolin-4(*3H*)-ones, as shown in Figure 3C. The molecular docking of 2-aryl quinazolin-4(*3H*)-one scaffold at the ATP binding site, has indicated that this scaffold occupies this cavity, and display several similar interactions like ATP, and known NLPR3 inflammasome inhibitors, MCC950 and β-estradiol. One of the key interaction (π-π stacking with Trp 416) of adenine moiety of ATP was found to be maintained by this new structural motif. Interestingly, this interaction was found to be common among known inflammasome inhibitors e.g. MCC950, acrylamide derivative [2-(2-chlorobenzyl)-*N*-(4-sulfamoylphenethyl)acrylamide].[11]

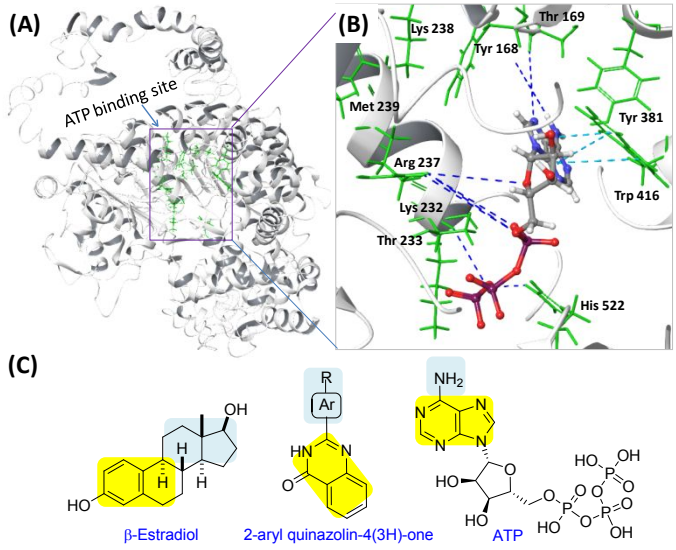

Figure 3. The homology model of NLRP3 inflammasome and design of its new inhibitors. **A**. homology model; **B**. binding site of the model showing interactions of ATP; **C**. designed "2-aryl quinazolin-4(*3H*)-one" scaffold.

Synthesis. Our synthetic efforts were initiated by examining the reaction of *O*-aminobenzamide **1a** with phenylacetylene **4a** using iodine as a catalyst and DMSO as a solvent by varying catalyst loading, temperature, reaction time and oxidant (Table 1). Reaction at room temperature produced desired 2-aryl quinazolin-4(*3H*)-one **2a**; however only in traces (entry 1). Under heating condition, in an open air atmosphere, the product **2a** was obtained in 28% yield (entry 2). When the molecular oxygen was employed, the yield of **2a** was improved up to 49% (entry 4). Further, on increasing the reaction temperature up to 140 °C, it has not positively impacted on the product yield (entry 5). On the use of iodine in stoichiometric equivalents, the **2a** yield was slightly improved, however along with the formation of iodo-byproduct **3a** (entries 6 and 7). Next, in order to reduce the formation of side product **3a**, reaction was then performed using catalytic amounts of I_2 and longer reaction time. These efforts have led to the identification of a optimized reaction condition, wherein, catalyst loading of 20 mol% I_2 using molecular oxygen at 110 °C for 16 h, produced 72% yield of desired product **2a** (entry 10). On lowering the reaction temperature to 80 °C, there was significant decrease in the product yield (**2a**, 20%; not shown in Table 1). Further investigation of other solvents such as DMF, toluene, ACN (entries 11-13), has shown that none of them are superior to DMSO, although all of them supported the progress of this reaction. Further, on addition of 1 equivalent of water to the optimized condition of entry 10, the desired product was formed in 70% yield, only after 12 h reaction time (entry 14). This condition was used for synthesis of quinazolin-4(*3H*)-one molecular library. Under this optimized condition, the desired quinazolin-4(*3H*)-one **2a** was obtained in equivalent yield, even after replacing the substrate phenylacetylene **4a** with styrene **5a**.

Table 1. Optimization of the Reaction Conditions[a]

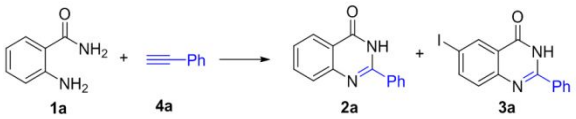

1a 4a 2a 3a

Entry	Iodine (mol%)	Solvent	Oxidant	temp (° C)	Time (h)	% yield[b] 2a	3a
1	10	DMSO	air	rt	10	traces	0
2	10	DMSO	air	110	10	28	0
3	10	DMSO	O_2	rt	10	18	0
4	10	DMSO	O_2	110	10	49	0
5	10	DMSO	O_2	140	10	48	0
6	150	DMSO	O_2	110	10	53	22
7	100	DMSO	O_2	110	10	53	20
8	70	DMSO	O_2	110	10	47	20
9	50	DMSO	O_2	110	16	62	13
10	20	DMSO	O_2	110	16	72	traces
11[c]	20	DMF	O_2	110	16	25	0
12[c]	20	Toluene	O_2	110	16	30	0
13[c]	20	ACN	O_2	110	16	20	0
14[d]	20	DMSO	O_2	110	12	70	traces

[a] *O*-aminobenzamide (1.0 mmol), phenylacetylene (1.2 mmol) and I_2 in DMSO stirred at a specified temperature; [b] isolated yield; [c] in case of entries 11-13, no reaction occurred when atmospheric air was used as oxidant; [d] addition of 1 equiv H_2O.

Using optimized reaction conditions, a series of 2-aryl quinazolin-4(*3H*)-ones were synthesized by varying aryl alkynes (Scheme 1). Phenylacetylenes substituted with various EDGs such as alkyls, OMe participated well in this reaction producing desired products in good yields (examples **2b-f**). Phenylacetylenes substituted with EWGs such as F, Br, CF_3, CN, and NO_2 also produced corresponding quinazolin-4(*3H*)-ones in good yields (examples **2g-k**). Further, the acetylenes with fused bicyclics and biphenyl rings (examples **2m** and **2n**) and heterocycles (example **2o**) also participated well in this reaction; however in the case of 9-ethynylanthracene, the desired product was obtained only in traces (example **2p**).[33] Unfortunately, aliphatic alkynes were not suitable for this kind of transformations under our optimized conditions. Furthermore, the reaction of **1a** with dimethyl acetylenedicarboxylate was also not successful.

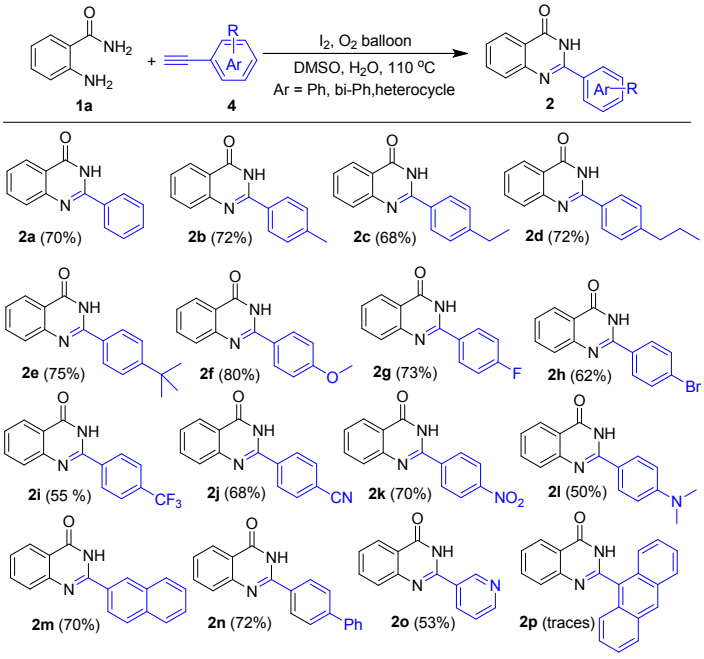

Scheme 1. Scope of the reaction for synthesis of various quinazolin-4(*3H*)-ones **2a-p**. Reagents and conditions: *O*-aminobenzamide (**1a**, 1.0 equiv.), phenylacetylene (**4**, 1.2 equiv.), 20 mol% I_2, DMSO, H_2O (1 equiv.) 110 °C, O_2 atmosphere, 12 h, 50-75%.

Similarly, the substrate scope was investigated with various substituted styrenes under optimized reaction conditions. The corresponding quinazolin-4(*3H*)-ones were obtained in good yield by varying the substitution on styrene precursor (Scheme 2). Styrenes substituted with EDGs (**2f**) as well as EWGs (**2g**, **2h**, **2k**, **2q**, **2r, 2s, 2t**) were well tolerated in this reaction. Biphenyl styrene (e.g. **2n**) as well as heterocyclic styrenes (e.g. **2o**, **2u**) also produced corresponding quinazolin-4(*3H*)-ones in good yields.

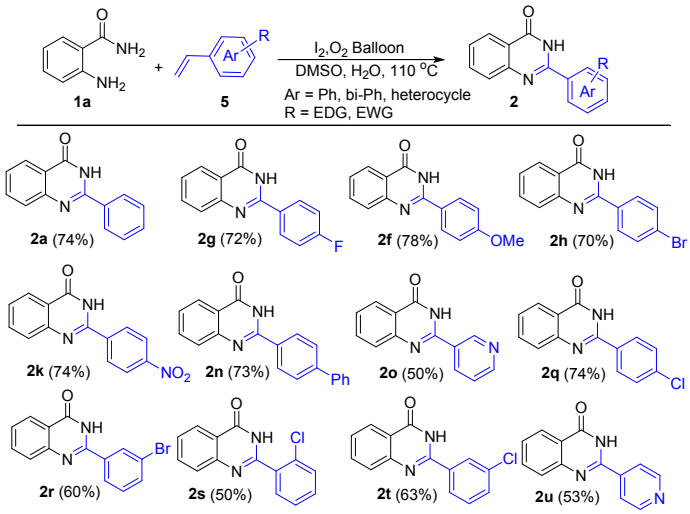

Scheme 2. Scope of the reaction for synthesis of various quinazolin-4(*3H*)-ones from *O*-aminobenzamide and styrenes. Reagents and conditions: *O*-aminobenzamide (**1a**, 1.0 equiv.), styrenes (**5**, 1.2 equiv.), 20 mol% I_2, DMSO, H_2O (1 equiv.) 110 °C, O_2 atmosphere, 12 h, 50-78%.

To further explore the scope of this reaction, various substituted 2-aminobenzamides were employed under optimal conditions. A series of halo groups on benzamide substrate such as chloro and iodo were well tolerated (examples **2v**-**2y**). In the case of 2-amino-*N*-ethylbenzamide, the desired quinazolin-4(*3H*)-one **2z** was not obtained. Next, we employed this protocol for preparation of pyrazolo[4,3-d]pyrimidin-7(6H)-one, which is another medicinally important highly privileged scaffold.[34] Using this protocol, pyrazolo[4,3-d]pyrimidin-7(*6H*)-one **6a** was prepared in 50% yield (Scheme 3). Interestingly, the internal alkyne as well as internal alkene also participated in this reaction, producing corresponding quinazolin-4(*3H*)-ones in 27-61% yields (Scheme 4).

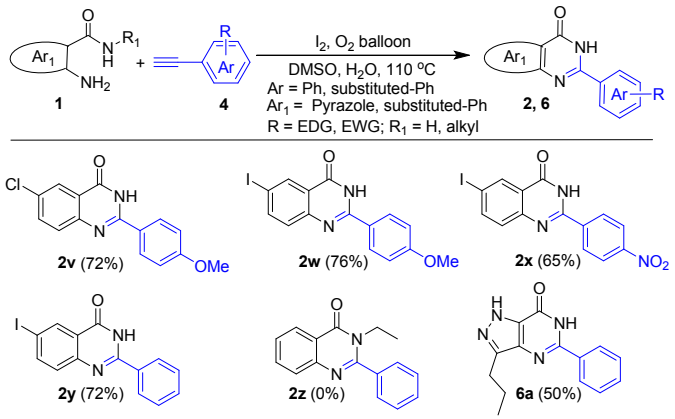

Scheme 3. Scope of the reaction for synthesis quinazolin-4(*3H*)-ones **2** and pyrazolo[4,3-*d*]pyrimidin-7(*6H*)-ones **6**. Reagents and conditions: *O*-aminobenzamide (**1**, 1.0 equiv.), phenylacetylenes (**4**, 1.2 equiv.), 20 mol% I_2, DMSO, H_2O, 110 °C, O_2 atmosphere, 12 h, 50-76%.

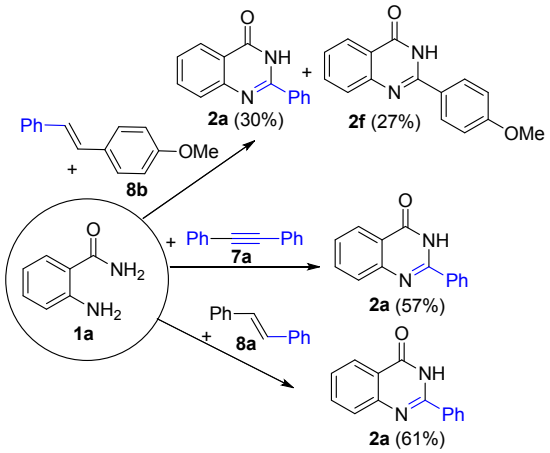

Scheme 4. Scope of the reaction for synthesis quinazolin-4(*3H*)-ones **2** using internal alkynes/ alkenes. Reagents and conditions: *O*-aminobenzamide (**1**, 1.0 equiv.), alkyne **7a**/ stilbene **8a-b** (1.2 equiv.), 20 mol% I_2, DMSO, H_2O, 110 °C, O_2 atmosphere, 12 h, 27-61%.

To gain mechanistic insights, a few control experiments were performed (Scheme 5A-E). In the presence of molecular oxygen, the reaction of α-iodophenylketone **9** with *O*-aminobenzamide **1a** produced 2-benzoyl quinazolin-4(*3H*)-one **10a** in good yield, both with I_2 (20 mol%) and without I_2 (Scheme 5A). These results indicated that α-iodophenylketone is very sensitive to DMSO-I_2 system which immediately forms phenylglyoxal **11** and leads to the formation of 2-

benzoyl product **10a**. Second control experiment was the condensation of phenylglyoxal **11** (1 mmol) and *O*-aminobenzamide **1a** (1 mmol) under molecular oxygen at 110 °C with catalytic amount of I_2. In this case also, we obtained 2-benzoyl product **10a** as a major product. However, in case of acetophenone **12** (1 mmol) using same reaction conditions, the desired quinazolin-4(*3H*)-one **2a** was obtained as a major product. In fourth experiment (Scheme 5D), reaction of *O*-aminobenzamide **1a** (1 mmol) with formaldehyde (3 mmol) in presence of molecular oxygen with 20 mol% I_2, produced quinazolin-4(*3H*)-one **13** (*m/z* 146) which we also observed as a byproduct during synthesis of all quinazolin-4(*3H*)-ones (based on MS analysis of reaction mixture; see Figure S1 of Supporting Information). Similarly, when *O*-aminobenzamide **1a** (1 mmol) was reacted with acetaldehyde (3 mmol) under optimized reaction conditions, the quinazolin-4(*3H*)-one **2a** was obtained (Scheme 5E).

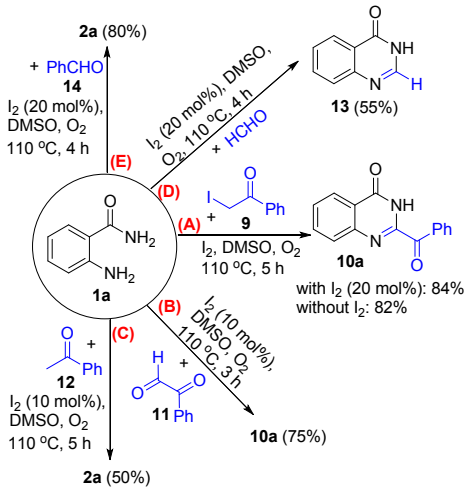

Scheme 5. Control experiments.

Accordingly, we proposed a plausible reaction mechanism for formation of **2a** from **1a** and **4a** as depicted in Figure 4. We propose two possible pathways. It is well known that under oxidative conditions, phenylacetylenes gets oxidized to α-iodophenylketone **9**[35] and acetophenones **12**.[36] In first path (Figure 4), phenylacetylene **4a** in the presence of I_2/DMSO gets converted to α-

iodophenylketone **9** which predominantly led to the formation of **10a** (Scheme 5B). In another pathway, phenylacetylene **4a** in the presence of I_2/DMSO gets converted to acetophenone **12** and facilitating the formation of intermediate **III** *via* formation of Schiff's base **II**. Intermediate **III** undergoes iodination to produce **IV**. The intermediate **III** gets converted to **V** *via* Kornblum type oxidation in the presence of DMSO.[37] Finally, the intermediate **V** undergoes HCHO elimination to produce iminium intermediate **VI**, which on deprotonation produces **2a**. Interestingly, a mass of *m/z* 146 for byproduct **13** [quinazolin-4(*3H*)-one] was observed when reaction mixture was monitored by ESI-MS. This clearly indicated that HCHO must be forming in-situ which leads to formation of **13** as a minor byproduct. Similarly, when internal alkyne **7a** (Scheme 4) was used, still the product **2a** was formed, *via* similar reaction mechanism. In this case, it is presumed that benzaldehyde **14** gets released which further on coupling with **1a**, produces same product **2a** (control experiment E, Scheme 5). This was also evidenced in case of stilbenes **8a** and **8b** (Scheme 4). The formation of 2-arylquinazolin-4(*3H*)-ones **2a** *via* condensation of *O*-aminobenzamide **1a** and styrene **5a** and stilbenes **8a-b** also occurs *via* iodine mediated conversion of styrene/ stilbene to corresponding acetophenone.[38]

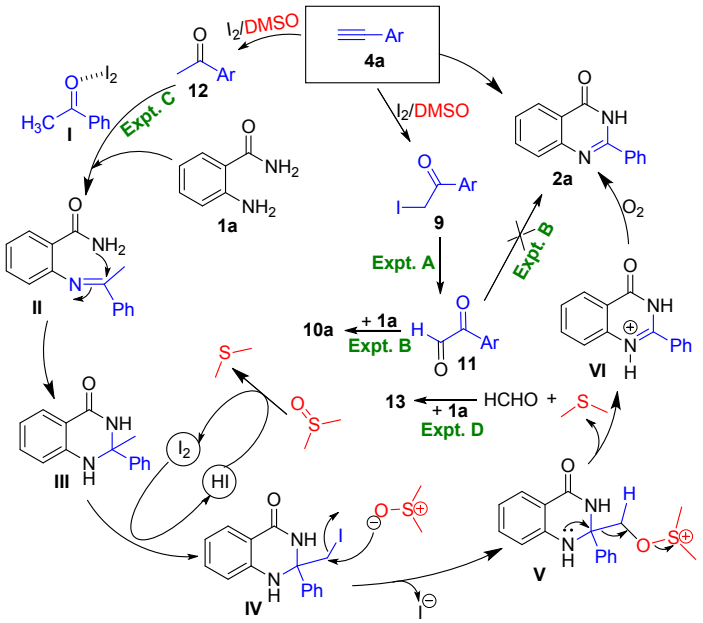

Figure 4. Plausible mechanism (control experiments from Scheme 5 are indicated here, in green colour) for formation of quinazolin-4(*3H*)-ones **2a** *via* condensation of *O*-aminobenzamide **1a** with phenylacetylene **4a**.

Inhibition of NLRP3 Inflammasome. For NLRP3 inhibition assay, mouse macrophages (J774A.1 cells) after priming with LPS were treated with 10 μM of test compound and were challenged with ATP (3 mM) for 30 min as a second signal. Activation of NLRP3 is culminated with the cleavage of pro-IL-1β into its activated form IL-1β. Compounds synthesized herein, and few quinazolin-4(*3H*)-ones prepared earlier **2aa-2ag**[30b] (in all, total 30 compounds; chemical structures of **2aa-2ag** are shown in Figure S2 of Supporting Information) were tested in this assay. The supernatant of vehicle/ test compound treated cells was collected and analyzed for IL-1β levels using ELISA. The results are shown in Table 2. Four compounds *viz*. **2f**, **2i**, **2k** and **2y** displayed significant suppression of IL-1β release in culture supernatant. Compound **2k** was the most active with 40% suppression of IL-1β release into the media. Further, in order to determine the IC_{50} value of compound **2k**, J774A.1 cells were treated with different concentrations (0.1- 10 μM) of quinazolin-4(*3H*)-one **2k**. A mild inhibitory effect was observed even at 1.25 μM; however, it showed maximum inhibition at a concentration of 10 μM. The IC_{50} of **2k** was found to be 5 μM.

Table 2. In-vitro inhibition of IL-1β release in J774A.1 cells by quinazolin-4(*3H*)-ones.[ab]

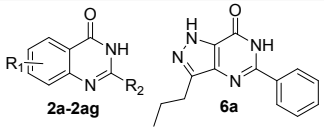 2a-2ag	6a	**% suppression of IL-1β release at 10 μM [mean ±SD]**	**Glide Score (ATP-binding site of NLRP3 inflammasome)**
Entry	**R_1**	**R_2**	
LPS + ATP + **2a**	H	Ph	12.7 ± 0.15	–6.60
LPS + ATP + **2f**	H	Ph (4-OMe)	28.8 ± 0.29	–8.50
LPS + ATP + **2i**	H	Ph (4-CF_3)	21.3 ± 0.10	–8.42
LPS + ATP + **2j**	H	Ph (4-CN)	13.9 ± 0.01	–7.66
LPS + ATP + **2k**	H	Ph (4-NO_2)	39.8 ± 0.11	–6.64
LPS + ATP + **2r**	H	Ph (3-Br)	16.1 ± 0.24	–6.63

LPS + ATP + **2t**	H	Ph (3-Cl)	12.9 ± 0.12	–6.90
LPS + ATP + **2y**	6-I	Ph	29.3 ± 0.12	–7.17
LPS + + ATP + MCC950[c]			105.8 ± 0.01	–8.05
LPS + DMSO + ATP[d]			0	-

[a]All compounds were dissolved in DMSO. J774A.1 cells after priming with LPS, were treated with compounds (10 μM) or vehicle (DMSO). Cells were then treated with ATP and the secretion of IL-1β in culture supernatants was measured by ELISA. [b]compounds **2b-2e**, **2g**, **2h**, **2l-2q**, **2s**, **2u-2x**, **2aa-2ag**, and **6a** showed ≤ 10% inhibition of IL-1β release at 10 μM, and thus these compounds are not listed in this table. [c]MCC950 was used as a positive control in this assay. [d]ATP treated cells without any test compound acts as a "control group".

Upon activation of NLRP3 inflammasome, the caspase-1 gets released which converts the pro IL-1β into its mature form IL-1β which is highly potent pro-inflammatory cytokine. Therefore, next we sought to investigate the effect of quinazolin-4(*3H*)-one **2k** on the expression of mature IL-1β in ATP-stimulated J774A.1 cells via western-blot analysis. As shown in Figure 5, the compound **2k** displayed dose-dependent decrease in the levels of cleaved IL-1β in the culture supernatant ($p < 0.005$). This study has further validated the results (Table 2) obtained in NLRP3 inflammasome activation assay.

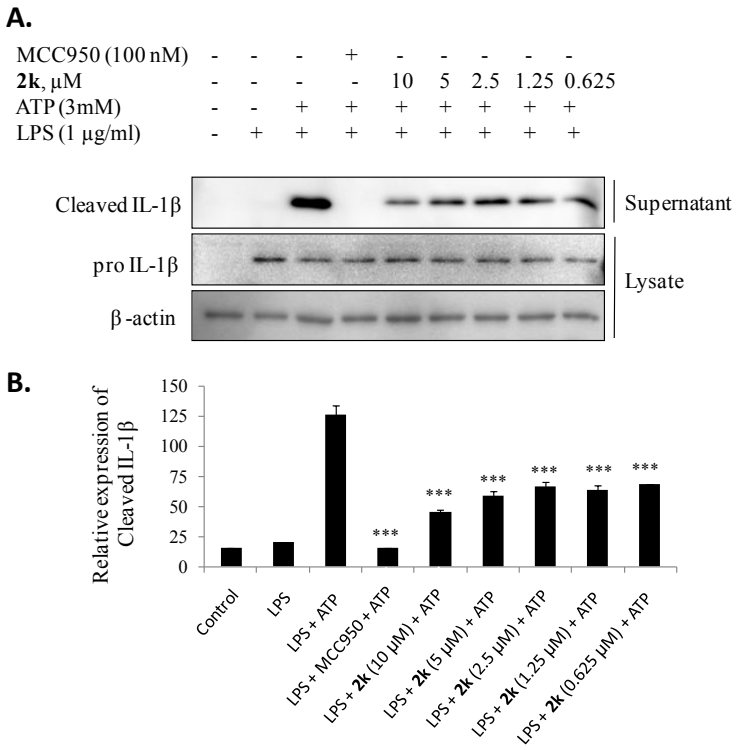

Figure 5. Western-blot analysis showing the effect of quinazolin-4(*3H*)-one **2k** on the expression of pro IL-1β and cleaved IL-1β in J774A.1 cells (statistical analysis was performed by comparing the test compound treated groups with "LPS+ATP" group. *p* value *** < 0.005).

To predict the putative binding mode of the quinazolin-4(*3H*)-one **2k**, the docking was performed with the developed homology model of NLRP3 inflammasome. The 3D-interaction map of **2k** is depicted in Figure 6B. The quinazolin-4(*3H*)-one ring displayed π- π interactions with Trp 416 residue, whereas the 3-phenyl ring showed π-π interactions with Tyr 381 residue of the active site. The nitro-functionality displayed additional cation-π (with Leu 171) and H-bonding interactions (with Thr 168, Thr 169). The known NLRP3 inflammasome inhibitor MCC950 strongly occupied the ATP binding cavity (glide score = –8.05) and displayed three π-π interactions and a H-bonding (*via* terminal OH group) with Trp 416 residue (Figure 6A). The other two active quinazolin-4(*3H*)-ones **2f** and **2i** were also found to occupy the ATP binding site

of NLRP3 inflammasome, and displayed interactions with Trp 416 and Tyr 381 residues (Figure S3 of Supporting Information).

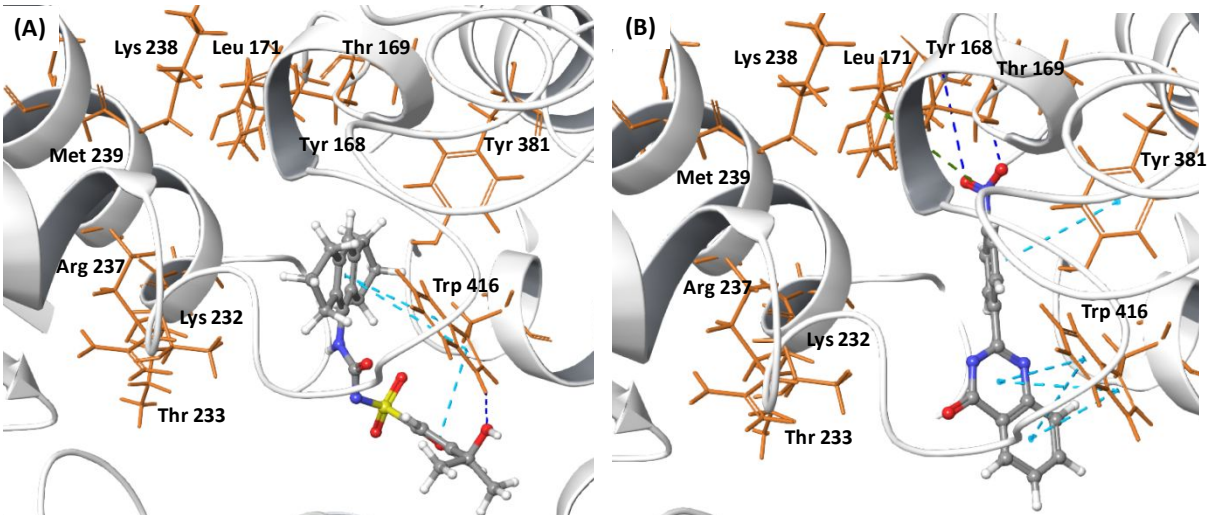

Figure 6. Interactions of MCC950 (A) and quinazolin-4(*3H*)-one **2k** (B) with ATP binding site of NLRP3 inflammasome. The light blue dotted lines indicate π-π interactions, dark blue as H-bonding and green-dotted lines as cation-π interactions.

CONCLUSION

Herein we have identified quinazolin-4(*3H*)-one as a new class of NLRP3 inflammasome inhibitors. The new method for synthesis of 2-aryl quinazolin-4(*3H*)-ones has also been developed *via* condensation of *O*-aminobenzamide with aryl alkynes/ alkenes using molecular oxygen as an oxidant. The quinazolin-4(*3H*)-one **2k** inhibited NLRP3 inflammasome with IC_{50} value of 5 μM. The molecular modelling study has indicated that it occupies the ATP binding site of the NLRP3 inflammasome. The promising NLRP3 inflammasome inhibitory activity of this new non-sulphonyl chemotype opens up an opportunity to investigate it further for its lead optimization and preclinical in-vivo validation.

EXPERIMENTAL SECTION

General. ^{1}H, ^{13}C and DEPT NMR spectra were recorded on FT-NMR 500 and 400 MHz instruments. Chemical data for protons are reported in parts per million (ppm) downfield from tetramethylsilane and are referenced to the residual proton in the NMR solvent ($CDCl_3$, 7.26 ppm; DMSO-d_6, 2.50 ppm). Carbon nuclear magnetic resonance spectra (^{13}C NMR) were recorded at 125 MHz or 100 MHz: chemical data for carbons are reported in parts per million (ppm, δ scale) downfield from referenced to the carbon resonance of the solvent ($CDCl_3$, 77 ppm; DMSO-d_6, 39.52 ppm). ESI-MS and HRMS spectra were recorded on Agilent 1100 LC-Q-TOF and HRMS-6540-UHD machines. IR spectra were recorded on Perkin-Elmer IR spectrophotometer. Melting points were recorded on digital melting point apparatus. The alkynes **4, 7a** and styrenes **5**, stilbenes **8a, 8b** used herein, were commercially procured from Sigma-Aldrich or TCI Chemicals.

For NLRP3 inflammasome assay, J774A.1 cell line was obtained from ECACC through Sigma-Aldrich. J774A.1 cells were cultured in Dulbecco's Modified Eagle's Medium (DMEM) supplemented with 10% fetal bovine serum (FBS, Life Technologies), 100U/ml penicillin and 100 mg/ml streptomycin (sigma). The reference standard MCC950 was purchased from Sigma-Aldrich (MO, USA).

Building the Homology Model of NLRP3 Inflammasome. The protein structure alignment of NACHT domain of the human NLRP3 protein (residues 220–536, Entry Id: Q96P20, Entry Name: NLRP3_HUMAN) was done with the resolved structure of NLRC4 (PDB ID: 4KXF), by multiple-thread alignments, as described by Zhang's research group through a web server (I-TASSER).[32] The obtained model was then subjected to the default protein preparation steps of Glide module of Schrodinger molecular modelling software. For docking, the highly conserved residue Lys 232 was considered and grid was prepared using 20 Å distance from this residue.

The developed model was validated by docking ATP and known inhibitors (MCC950[12a], 2-(2-chlorobenzyl)-*N*-(4-sulfamoylphenethyl)acrylamide[11]) of NLRP3 inflammasome.

Optimized Procedure for Preparation of 2-Aryl Quinazolin-4(*3H*)-ones (2) and Pyrazolo[4,3-D]pyrimidin-7(6H)-ones (6). The reaction mixture of alkyne or alkene (**4** or **5**, 1.2 equiv) and iodine (0.2 equiv) in DMSO and H_2O (1 equiv) under molecular oxygen at 110 ^oC was stirred for 20 min. Then corresponding 2-aminobenzamides (**1**, 1 equiv.) or 4-amino-1-methyl-3-propyl-1H-pyrazole-5-carboxamide (1 equiv) was added and the reaction mixture was stirred further for 12 h. After completion of the reaction, water (20 mL) was added to the reaction mixture. A saturated $Na_2S_2O_3$ solution was then added until the brown color disappeared. Product was extracted with EtOAc (3 × 10 mL). The organic layer was collected, dried on anhydrous sodium sulphate and solvent was evaporated on rotary evaporator to get the crude product. The crude product was purified by silica gel (#100-200) column chromatography using 2 to 20% EtOAc: hexane to get pure quinazolin-4(*3H*)-ones. Most of the compounds were purified without column chromatography. For this, the MeOH was added to the crude product and the resulting suspension was filtered. Obtained residue was washed with MeOH (2-3 times) and dried. To get good yield of the product, on addition of methanol, the product was allowed to settle down for 2-3 days, which results in formation of a crystalline pure product.

*2-Phenylquinazolin-4(3H)-one (**2a**)*.[28a,39] White solid. yield: 70% (114 mg). m.p. 232-235 °C. ^{1}H NMR (400 MHz, DMSO-d_6, ppm): δ 11.57 (s, 1H), 8.34 (d, *J* = 7.8 Hz, 1H), 8.26 - 8.24 (m, 2H), 7.86-7.80 (m, 2H), 7.60-7.50 (m, 3H), 7.52 (t, *J* = 7.2 Hz, 1H). ^{13}C{^{1}H} NMR (101 MHz, $CDCl_3$, ppm): δ 163.9, 151.9, 149.5, 134.9, 132.8, 131.6, 129.0, 127.9, 127.4, 126.8, 126.3, 120.8. IR ($CHCl_3$): ν_{max} 3436, 2926, 1666, 1481, 1297, 1144 cm^{-1}. ESI-MS: *m/z* 223.08 $[M+H]^+$. HRMS (ESI-TOF) m/z: $[M+H]^+$ Calcd for $C_{14}H_{11}N_2O$ 223.0871; Found 223.0869.

*2-(p-Tolyl)quinazolin-4(3H)-one (**2b**)*.[28a,39] White solid. yield: 72% (124 mg). m.p. 239-242 °C. ^{1}H NMR (400 MHz, DMSO-d_6, ppm): δ 8.16 (d, *J* = 8.0 Hz, 1H), 8.11 (d, *J* = 8.0 Hz, 2H), 7.84 (t, *J* = 8.2 Hz, 1H), 7.75 (d, *J* = 7.8 Hz, 1H), 7.52 (t, *J* = 8.2 Hz, 1H), 7.38 (d, *J* = 8.0 Hz, 2H), 2.40 (s, 3H). ^{13}C{^{1}H} NMR (101 MHz, DMSO-d_6, ppm): δ 162.7, 152.7, 149.5, 149.3, 144.9, 135.1, 130.3, 129.6, 128.1, 127.9, 126.9, 126.3, 121.3, 21.5. IR ($CHCl_3$): ν_{max} 3436, 2918, 1667, 1600, 1486, 1241 cm^{-1}. ESI-MS: *m/z* 237.10 $[M+H]^+$. HRMS (ESI-TOF) m/z: $[M+H]^+$ Calcd for $C_{15}H_{13}N_2O$ 237.1022; Found 237.1029.

*2-(4-Ethylphenyl)quinazolin-4(3H)-one (**2c**)*.[22a] White solid. yield: 68% (125 mg). m.p. 205-207 °C. ^{1}H NMR (400 MHz, $CDCl_3$, ppm): δ 8.27 (d, *J* = 7.9 Hz, 1H), 7.98 (d, *J* = 8.0 Hz, 2H), 7.83-7.81 (m, 1H), 7.52-7.49 (m, 1H), 7.39 (d, *J* = 8.0 Hz, 2H), 7.33 (m, 1H), 2.76 (q, *J* = 8.0, 12.0 Hz, 2H), 1.29 (t, *J* = 8.0 Hz, 3H). ^{13}C{^{1}H} NMR (101 MHz, DMSO-d_6, ppm): δ 162.8, 152.7, 149.3, 148.1, 135.1, 130.6, 128.5, 128.3, 127.9, 126.9, 126.3, 121.4, 28.5, 15.8. IR ($CHCl_3$): ν_{max} 3436, 2920, 1669, 1612, 1482, 1240 cm^{-1}. ESI-MS: *m/z* 251.11 $[M+H]^+$. HRMS (ESI-TOF) m/z: $[M+H]^+$ Calcd for $C_{16}H_{15}N_2O$ 251.1179; Found 251.1201.

*2-(4-Propylphenyl)quinazolin-4(3H)-one (**2d**)*. White solid. yield: 72% (139 mg). m.p. 200-202 °C. ^{1}H NMR (400 MHz, DMSO-d_6, ppm): δ 12.50 (s, 1H), 8.16 - 8.11 (m, 3H), 7.84 (t, *J* = 8.2 Hz, 1H), 7.74 (d, *J* = 7.9 Hz, 1H), 7.52 (t, *J* = 7.0 Hz, 1H), 7.38 (d, *J* = 8.2 Hz, 2H), 2.65 (t, *J* = 7.5 Hz, 2H), 1.69 -1.62 (m, 2H), 0.92 (t, *J* = 7.3 Hz, 3H). ^{13}C{^{1}H} NMR (126 MHz, $CDCl_3$, ppm): δ 163.7, 151.8, 149.6, 147.0, 134.9, 130.1, 129.3, 127.9, 127.2, 126.5, 126.3, 120.8, 38.2, 24.4, 14.0. IR ($CHCl_3$): ν_{max} 3436, 2918, 1667, 1600, 1486, 1241 cm^{-1}. ESI-MS: *m/z* 265.12 $[M+H]^+$. HPLC purity: 92% (t_R = 14.4 min).

*2-(4-(Tert-butyl)phenyl)quinazolin-4(3H)-one (**2e**)*.[28a] White solid. yield: 75% (153 mg). m.p. 233-235 °C. ^{1}H NMR (400 MHz, $CDCl_3$, ppm): δ 10.85 (s, 1H), 8.34 (d, *J* = 7.7 Hz, 1H), 8.12

(d, *J* = 8.0 Hz, 2H), 7.85-7.78 (m, 2H), 7.60 (d, *J* = 8.0 Hz, 2H), 7.52 (t, *J* = 8.0 Hz, 1H), 1.39 (s, 9H). $^{13}C\{^{1}H\}$ NMR (126 MHz, $CDCl_3$, ppm): δ 163.1, 154.8, 151.1, 134.4, 129.3, 127.4, 126.5, 126.1, 125.9, 125.6, 120.3, 34.5, 30.7. IR ($CHCl_3$): ν_{max} 3436, 2918, 1667, 1600, 1486, 1241 cm^{-1}. ESI-MS: *m/z* 279.14 $[M+H]^+$. HRMS (ESI-TOF) m/z: $[M+H]^+$ Calcd for $C_{18}H_{19}N_2O$ 279.1492; Found 279.1491.

*2-(4-Methoxyphenyl)quinazolin-4(3H)-one (**2f**).*[28a,39] White solid. yield: 80% (148 mg). m.p. 247-249 °C. ^{1}H NMR (400 MHz, $CDCl_3$, ppm): δ 8.27 (d, *J* = 7.8 Hz, 1H), 8.07 (d, *J* = 8.0 Hz, 2H), 7.79 (d, *J* = 4.0 Hz, 2H), 7.49 (m, 1H), 7.08 (d, *J* = 12.0 Hz, 2H), 3.91 (s, 3H). $^{13}C\{^{1}H\}$ NMR (126 MHz, DMSO-d_6 + $CDCl_3$, ppm): δ 162.3, 161.8, 151.8, 148.9, 134.5, 129.4, 127.2, 126.1, 125.8, 124.7, 120.6, 114.0, 55.4. IR ($CHCl_3$): ν_{max} 3436, 2920, 1678, 1600, 1484, 1031 cm^{-1}. ESI-MS: *m/z* 253.09 $[M+H]^+$. HRMS (ESI-TOF) m/z: $[M+H]^+$ Calcd for $C_{15}H_{13}N_2O_2$ 253.0972; Found 253.0967.

*2-(4-Fluorophenyl)quinazolin-4(3H)-one (**2g**).*[28a,29] White solid. yield: 73% (128 mg). m.p. 240-242 °C. ^{1}H NMR (400 MHz, DMSO-d_6, ppm): δ 12.58 (s, 1H), 8.26 (dd, *J* = 4.0, 8.0 Hz, 2H), 8.16 (d, *J* = 8.0 Hz, 1H), 7.84 (t, *J* = 8.0 Hz, 1H), 7.75 (d, *J* = 8.0 Hz, 1H), 7.53 (t, *J* = 8.0 Hz, 1H), 7.40 (t, *J* = 8.0 Hz, 2H). $^{13}C\{^{1}H\}$ NMR (126 MHz, DMSO-d_6, ppm): δ 163.5 (d, $^{1}J_{CF}$ = 103 Hz), 151.8, 149.1, 135.1, 130.9 (d, $^{2}J_{CF}$ = 8.8 Hz), 129.7, 127.9, 127.1, 126.3, 121.4, 116.2, 116.0. IR ($CHCl_3$): ν_{max} 3424, 2922, 2852, 2853, 1672, 1466, 1288, 1095 cm^{-1}. ESI-MS: *m/z* 241.07 $[M+H]^+$. HRMS (ESI-TOF) m/z: $[M+H]^+$ Calcd for $C_{14}H_{10}FN_2O$ 241.0772; Found 241.0782.

*2-(4-Bromophenyl)quinazolin-4(3H)-one (**2h**).*[22d,40] White solid. yield: 62% (136 mg). m.p. 292-295 °C. ^{1}H NMR (400 MHz, DMSO-d_6, ppm): δ 12.66 (s, 1H), 8.21-8.16 (m, 3H), 7.88 (d, *J* = 8.0 Hz, 1H), 7.80-7.78 (m, 3H), 7.58 (t, *J* = 7.3 Hz, 1H). $^{13}C\{^{1}H\}$ NMR (126 MHz, DMSO-d_6, ppm): δ 162.6, 151.9, 149.1, 135.2, 132.4, 132.1, 130.3, 128.0, 125.7, 121.5. IR ($CHCl_3$): ν_{max}

3428, 2919, 1659, 1633, 1335, 1179 cm^{-1}. ESI-MS: *m/z* 300.98 $[M+H]^+$. HRMS (ESI-TOF) m/z: $[M+H]^+$ Calcd for $C_{14}H_{10}{}^{81}BrN_2O$ 302.9951; Found 302.9945.

*2-(4-(Trifluoromethyl)phenyl)quinazolin-4(3H)-one (**2i**).*[28a] White solid. yield: 55% (117 mg). m.p. 280-282 °C. ^1H NMR (400 MHz, DMSO-d_6, ppm) δ 12.77 (s, 1H), 8.37 (d, *J* = 8.1 Hz, 2H), 8.18 (d, *J* = 7.0 Hz, 1H), 7.93 (d, *J* = 8.3 Hz, 2H), 7.87 (t, *J* = 7.6 Hz, 1H), 7.78 (d, *J* = 8.0 Hz, 1H), 7.57 (t, *J* = 7.2 Hz, 1H). $^{13}C\{^1H\}$ NMR (101 MHz, DMSO-d_6, ppm) δ 162.6, 151.7, 148.9, 137.1, 135.2, 131.8 (d, $^2J_{CF}$ = 32 Hz), 129.2, 128.1, 127.6, 126.4, 126.0 (d, $^3J_{CF}$ = 3 Hz), 125.8 (d, $^1J_{CF}$ = 273 Hz), 121.7. IR ($CHCl_3$): ν_{max} 3428, 2919, 1659, 1633, 1335, 1179 cm^{-1}. ESI-MS: *m/z* 291.07 $[M+H]^+$. HRMS (ESI-TOF) m/z: $[M+H]^+$ Calcd for $C_{15}H_{10}F_3N_2O$ 291.0740; Found 291.0726.

*2-(4-(Cyano)phenyl)quinazolin-4(3H)-one (**2j**).*[24,40] White solid. yield: 68% (123 mg). m.p. 280-282 °C. ^1H NMR (400 MHz, DMSO-d_6, ppm): δ 12.75 (s, 1H), 8.34 (t, *J* = 8.0 Hz, 2H), 8.20 (d, *J* = 8.0 Hz, 1H), 8.06 (d, *J* = 8.0 Hz, 1H), 7.95-7.78 (m, 3H), 7.58 (t, *J* = 8.0 Hz, 1H). IR ($CHCl_3$): ν_{max} 3428, 2919, 1659, 1633, 1335, 1179 cm^{-1}. ESI-MS: *m/z* 248.08 $[M+H]^+$. HRMS (ESI-TOF) m/z: $[M+H]^+$ Calcd for $C_{15}H_{10}N_3O$ 248.0818; Found 248.0817.

*2-(4-Nitrophenyl)quinazolin-4(3H)-one (**2k**).*[41] Yellow solid. yield: 70% (137 mg). m.p. >300 °C. ^1H NMR (400 MHz, DMSO-d_6, ppm): δ 12.84 (s, 1H), 8.40 (m, 4H), 8.19 (d, *J* = 4.0 Hz, 1H), 7.88 (t, *J* = 7.6 Hz, 1H), 7.80 (d, *J* = 7.9 Hz, 1H), 7.59 (t, *J* = 7.4 Hz, 1H). $^{13}C\{^1H\}$ NMR (101 MHz, DMSO-d_6, ppm): δ 162.6, 151.1, 149.5, 148.8, 139.1, 136.3, 135.3, 129.8, 129.2, 127.9, 126.4, 124.1, 121.7. IR ($CHCl_3$): ν_{max} 3410, 2921, 1681, 1517, 1470, 1351, 1020 cm^{-1}. ESI-MS: *m/z* 266.05 $[M-H]^-$. HRMS (ESI-TOF) m/z: $[M-H]^-$ Calcd for $C_{14}H_8N_3O_3$ 266.0571; Found 266.0580.

*2-(4-(Dimethylamino)phenyl)quinazolin-4(3H)-one (**2l**).*[42] White solid. yield: 50% (97 mg). m.p. > 300° C. ^{1}H NMR (400 MHz, $CDCl_3$, ppm): δ 9.98 (s, 1H), 8.29 (d, *J* = 7.9 Hz, 1H), 8.01 (d, *J* = 8.0 Hz, 2H), 7.76 (d, *J* = 4.0 Hz, 2H), 7.44-7.40 (m, 1H), 6.80 (d, *J* = 8.0 Hz, 2H), 3.08 (s, 6H). ^{13}C{^{1}H} NMR (126 MHz, $CDCl_3$, ppm): δ 163.0, 152.6, 151.5, 150.0, 134.6, 128.1, 127.5, 126.4, 125.7, 120.4, 119.2, 111.7, 40.1. IR ($CHCl_3$): ν_{max} 3301, 2922, 1595, 1580, 1441, 1106, 1019 cm^{-1}. ESI-MS: *m/z* 266.12 $[M+H]^+$. HRMS (ESI-TOF) m/z: $[M+H]^+$ Calcd for $C_{16}H_{16}N_3O$ 266.1288; Found 266.1275.

*2-(Naphthalen-2-yl)quinazolin-4(3H)-one (**2m**).*[28a] White solid. yield: 70% (140 mg). m.p. 247 - 249 °C. ^{1}H NMR (500 MHz, DMSO-d_6, ppm): δ 12.35 (s, 1H), 8.48 (d, *J* = 8.3 Hz, 1H), 8.29-8.24 (q, *J* = 8.0, 12.0 Hz, 2H), 8.16-8.11 (q, *J* = 8.0, 12.0 Hz, 2H), 7.86 (t, *J* = 8.0 Hz, 1H), 7.69-7.65 (m, 5H). ^{13}C{^{1}H} NMR (126 MHz, DMSO-d_6, ppm): δ 161.6, 150.5, 147.7, 135.2, 134.3, 133.8, 133.2, 131.7, 130.9, 129.3, 129.1, 128.9, 128.8, 127.2, 126.5, 125.3, 125.1, 123.4. IR ($CHCl_3$): ν_{max} 3356, 2920, 1666, 1574, 1443, 1292, 1022 cm^{-1}. ESI-MS: *m/z* 273.10 $[M+H]^+$. HRMS (ESI-TOF) m/z: $[M+H]^+$ Calcd for $C_{18}H_{13}N_2O$ 273.1022; Found 273.1040.

*2-([1,1'-Biphenyl]-4-yl)quinazolin-4(3H)-one (**2n**).*[25] White solid. yield: 72% (157 mg). m.p. 266-269 °C. ^{1}H NMR (400 MHz, DMSO-d_6, ppm): δ 12.62 (s, 1H), 8.32 (d, *J* = 8.0 Hz, 2H), 8.19 (d, *J* = 8.0 Hz, 1H), 7.89-7.84 (m, 3H), 7.80-7.77 (m, 3H), 7.56-7.51 (m, 3H), 7.45 (m, 1H). ^{13}C{^{1}H} NMR (126 MHz, DMSO+10% $CDCl_3$, ppm): δ 162.2, 151.9, 148.7, 142.8, 138.9, 134.6, 131.5, 129.0, 128.3, 127.4, 126.8, 126.7, 126.5, 125.8, 120.9. IR ($CHCl_3$): ν_{max} 3585, 2921, 1673, 1467, 1169 cm^{-1}. ESI-MS: *m/z* 299.11 $[M+H]^+$. HRMS (ESI-TOF) m/z: $[M+H]^+$ Calcd for $C_{20}H_{15}N_2O$ 299.1179; Found 299.1174.

*2-(Pyridin-3-yl)quinazolin-4(3H)-one (**2o**).*[39] White solid. yield: 65% (90 mg). m.p. 270-273 °C. ^{1}H NMR (400 MHz, DMSO-d_6, ppm): δ 12.75 (s, 1H), 9.30 (s, 1H), 8.76 (d, *J* = 4.7 Hz,

1H), 8.51 (d, *J* = 8.0 Hz, 1H), 8.19 (d, *J* = 7.9 Hz, 1H), 7.87 (t, *J* = 7.6 Hz, 1H), 7.78 (d, *J* = 8.1 Hz, 1H), 7.62-7.51 (m, 2H). $^{13}C\{^1H\}$ NMR (101 MHz, DMSO-d_6, ppm): δ 162.6, 152.3, 151.2, 149.0, 135.9, 135.2, 129.2, 128.1, 127.4, 126.4, 124.0, 121.6. IR ($CHCl_3$): ν_{max} 3585, 2921, 1673, 1467, 1169 cm^{-1}. ESI-MS: *m/z* 224.07 $[M+H]^+$. HPLC purity: 93% (t_R = 5.6 min).

*2-(4-Chlorophenyl)quinazolin-4(3H)-one (**2q**).*[29,39] White solid. yield: 74% (140 mg). m.p. 295-297 °C. ^1H NMR (400 MHz, DMSO-d_6, ppm) δ 12.59 (s, 1H), 8.18-8.11 (m, 3H), 7.83-7.79 (m, 1H), 7.71 (d, *J* = 7.7 Hz, 1H), 7.61 (d, *J* = 8.7 Hz, 2H), 7.59-7.43 (t, *J* = 8.0 Hz, 1H). $^{13}C\{^1H\}$ NMR (126 MHz, DMSO-d_6, ppm) δ 162.7, 151.9, 149.0, 136.8, 135.2, 132.0, 130.1, 129.2, 127.9, 127.3, 126.3, 121.4. IR ($CHCl_3$): V_{max} 3584, 3393, 2922, 2851, 2346, 1705, 1674, 1346, 1017 cm^{-1}. ESI-MS: *m/z* 257.0953 $[M+H]^+$. HRMS (ESI-TOF) m/z: $[M+H]^+$ Calcd for $C_{14}H_{10}ClN_2O$ 257.0476; Found 257.0477.

*2-(3-Bromophenyl)quinazolin-4(3H)-one (**2r**).*[43] White solid. yield: 60% (132 mg). m.p. 295-297 °C. ^1H NMR (400 MHz, DMSO-d_6, ppm) δ 12.63 (s, 1H), 8.38 (brs, 1H), 8.17 (t, *J* = 12 Hz, 2H), 7.86 (t, *J* = 4.0 Hz, 1H), 7.78 (t, *J* = 12 Hz, 2H), 7.57-7.50 (dd, *J* = 8.0, 20 Hz, 2H). $^{13}C\{^1H\}$ NMR (101 MHz, DMSO-d_6, ppm) δ 162.6, 151.4, 148.9, 135.4, 135.2, 134.5, 131.2, 130.9, 128.1, 127.4, 127.3, 126.4, 122.4, 121.6. IR ($CHCl_3$): ν_{max} 3396, 2921, 2851, 2353, 1680, 1606 cm^{-1}. ESI-MS: *m/z* 300.9 $[M+H]^+$. HRMS (ESI-TOF) m/z: $[M+H]^+$ Calcd for $C_{14}H_{10}BrN_2O$ 300.9971; Found 300.9964.

*2-(2-Chlorophenyl)quinazolin-4(3H)-one (**2s**).*[44] White solid. yield; 50% (95 mg). m.p. 196-198 °C. ^1H NMR (400 MHz, DMSO-d_6, ppm) δ 12.36 (s, 1H), 8.17 (d, *J* = 12 Hz, 2H), 8.09 (m, 1H), 7.78-7.76 (m, 1H), 7.66 (d, *J* = 7.8 Hz, 1H), 7.45-7.43 (m, 1H), 7.07 (d, *J* = 8.0 Hz, 2H). $^{13}C\{^1H\}$ NMR (101 MHz, DMSO-d_6, ppm) δ 161.9, 152.7, 149.1, 135.1, 134.3, 132.1, 132.0, 131.4, 130.1, 128.0, 127.7, 127.6, 126.3, 121.7. IR ($CHCl_3$): ν_{max} 3584, 3405, 2923, 2852,

1686, 1117 cm^{-1}. ESI-MS: *m/z* 257.0973 $[M+H]^+$. HRMS (ESI-TOF) m/z: $[M+H]^+$ Calcd for $C_{14}H_{10}ClN_2O$ 257.0476; Found 257.0474; HPLC purity: 93% (t_R = 10.8 min).

*2-(3-Chlorophenyl)quinazolin-4(3H)-one (**2t**).*[40] White solid. yield; 63% (120 mg). m.p. 252-254 °C. ^1H NMR (400 MHz, DMSO-d_6, ppm) δ 12.58 (s, 1H), δ 8.20 (dd, *J* = 5.3, 11.2 Hz, 1H), 8.11 (m, 1H), 7.86-7.79 (m, 1H), 7.73 (d, *J* = 7.8 Hz, 1H), 7.65-7.61 (m, 1H), 7.58-7.48 (m, 2H). $^{13}C\{^1H\}$ NMR (126 MHz, DMSO-d_6, ppm) δ 162.6, 151.4, 149.1, 135.2, 133.9, 131.6, 131.0, 128.0, 127.4, 126.9, 126.4, 121.6. IR ($CHCl_3$): ν_{max} 3584, 3405, 2923, 2852, 1686, 1117 cm^{-1}. ESI-MS: *m/z* 257.0973. HPLC purity: 98% (t_R = 12.7 min).

*2-(Pyridin-4-yl)quinazolin-4(3H)-one (**2u**).*[40] white solid. yield: 53% (87 mg). m.p. 281-284 °C. ^1H NMR (400 MHz, DMSO-d_6, ppm) δ 8.80 (d, *J* = 5.8 Hz, 2H), 8.19 (d, *J* = 7.6 Hz, 1H), 8.13 (d, *J* = 6.0 Hz, 2H), 7.87 (t, *J* = 7.6 Hz, 1H), 7.80 (d, *J* = 8.1 Hz, 1H), 7.58 (t, *J* = 7.5 Hz, 1H). $^{13}C\{^1H\}$ NMR (101 MHz, DMSO-d_6, ppm): 162.8, 151.4, 150.7, 148.8, 140.7, 135.2, 128.2, 127.8, 126.4, 122.1, 122.0. IR ($CHCl_3$): ν_{max} 3417, 2919, 1650, 1506, 1485, 1224, 1149 cm^{-1}. ESI-MS: *m/z* 224.1 $[M+H]^+$. HRMS (ESI-TOF) m/z: $[M+H]^+$ Calcd for $C_{13}H_{10}IN_3O$ 224.0818; Found 224.0796. HPLC purity: 99.8% (t_R = 5.1 min).

*6-Chloro-2-(4-methoxyphenyl)quinazolin-4(3H)-one (**2v**).*[39] White solid. yield: 72% (121 mg). m.p. 286-288 °C. ^1H NMR (400 MHz, DMSO-d_6, ppm): δ 12.83 (s, 1H), 8.20-8.14 (m, 3H), 7.92 (dd, *J* = 4.0, 12.0 Hz, 1H), 7.82 (d, *J* = 8.7 Hz, 1H), 7.14 (d, *J* = 8.8 Hz, 2H), 3.90 (s, 3H). IR ($CHCl_3$): ν_{max} 3418, 2924, 1682, 1651, 1460, 1263, 1127 cm^{-1}. ESI-MS: *m/z* 287.05 $[M+H]^+$. HRMS (ESI-TOF) m/z: $[M+H]^+$ Calcd for $C_{15}H_{12}ClN_2O_2$ 287.0582; Found 287.0583.

*6-Iodo-2-(4-methoxyphenyl)quinazolin-4(3H)-one (**2w**).* White solid. yield: 76% (109 mg). m.p. 220-222 °C. ^1H NMR (400 MHz, DMSO-d_6, ppm): δ 12.81 (s, 1H), 8.48 (d, *J* = 4.0 Hz, 1H), 8.17 (m, 3H), 7.57 (d, *J* = 8.0 Hz, 1H), 7.14 (d, *J* = 12 Hz, 2H), 3.89 (s, 3H). $^{13}C\{^1H\}$ NMR

(126 MHz, DMSO-d_6, ppm): δ 185.6, 164.8, 160.4, 150.5, 146.9, 143.5, 134.8, 133.9, 126.9, 124.9, 114.5, 56.2; IR $CHCl_3$): ν_{max} 3418, 2920, 1658, 1457, 1313, 1167 cm^{-1}. ESI-MS: *m/z* 378.99 $[M+H]^+$. HRMS (ESI-TOF) m/z: $[M+H]^+$ Calcd for $C_{15}H_{12}IN_2O_2$ 378.9938; Found 378.9928.

*6-Iodo-2-(4-nitrophenyl)quinazolin-4(3H)-one (**2x**).* White solid. yield: 65% (97 mg). m.p. > 260 °C. ^1H NMR (400 MHz, DMSO-d_6, ppm): δ 12.92 (s, 1H), 8.50 (d, *J* = 4.0 Hz, 1H), 8.48 - 8.38 (m, 4H), 8.20 (dd, *J* = 1.9, 8.5 Hz, 1H), 7.58 (d, *J* = 8.0 Hz, 1H). $^{13}C\{^1H\}$ NMR (126 MHz, $CDCl_3$ + DMSO-d_6, ppm): δ 185.8, 159.9, 150.0, 148.2, 146.1, 143.2, 139.2, 134.3, 132.2, 130.5, 124.5, 123.1. IR ($CHCl_3$): ν_{max} 3426, 2918, 1666, 1519, 1342, 1160, 1016 cm^{-1}. HRMS (ESI-TOF) m/z: $[M-H]^-$ Calcd for $C_{14}H_7IN_3O_3$ 391.9538; Found 391.9521.

*6-Iodo-2-phenylquinazolin-4(3H)-one (**2y**).* White solid. yield: 72% (95 mg). m.p. > 260 °C. ^1H NMR (400 MHz, DMSO-d_6, ppm): δ 12.87 (s, 1H), 8.49 (d, *J* = 4.0 Hz, 1H), 8.20-8.15 (m, 3H), 7.76 (t, *J* = 7.4 Hz, 1H), 7.62-7.56 (q, *J* = 8.0, 16.0 Hz, 3H). $^{13}C\{^1H\}$ NMR (126 MHz, DMSO-d_6 + 10% $CDCl_3$, ppm): δ 187.0, 143.1, 142.9, 134.3, 134.1, 133.9, 131.6, 130.8, 128.6, 128.5, 127.8, 124.5, 122.6, 94.2. IR ($CHCl_3$): ν_{max} 3397, 2921, 1662, 1591, 1285, 1173 cm^{-1}. ESI-MS: *m/z* 348.98 $[M+H]^+$. HRMS (ESI-TOF) m/z: $[M+H]^+$ Calcd for $C_{14}H_{10}IN_2O$ 348.9832; Found 348.9822.

*1-Methyl-5-phenyl-3-propyl-1,6-dihydro-7H-pyrazolo[4,3-d]pyrimidin-7-one (**6a**).*[24] White solid. yield: 50% (73 mg). m.p.194-197 °C. ^1H NMR (400 MHz, $CDCl_3$, ppm): δ 10.91 (s, 1H), 8.11 (dd, *J* = 3.1, 6.5 Hz, 2H), 7.54 (d, *J* = 2.0 Hz, 3H), 4.30 (s, 3H), 2.98-2.92 (m, 2H), 1.91-1.85 (m, 2H), 1.04 (t, *J* = 7.3 Hz, 3H). $^{13}C\{^1H\}$ NMR (101 MHz, $CDCl_3$, ppm): δ 155.3, 149.0, 146.4, 138.8, 132.4, 130.5, 128.3, 126.6, 124.8, 37.6, 27.2, 21.8, 13.5. IR ($CHCl_3$): ν_{max} 3440,

2931, 1688, 1633, 1490, 1100 cm^{-1}. ESI-MS: *m/z* 269.14 $[M+H]^+$. HRMS (ESI-TOF) m/z: $[M+H]^+$ Calcd for $C_{15}H_{17}N_4O$ 269.1397; Found 269.1389.

*2-Benzoylquinazolin-4(3H)-one (**10a**).*[45] White solid. yield: 84% (154 mg). m.p. 179-182 °C. ^1H NMR (400 MHz, $CDCl_3$, ppm): δ 10.18 (s, 1H), 8.52 (d, *J* = 8.0 Hz, 2H), 8.41 (d, *J* = 8.0 Hz, 1H), 7.95 (d, *J* = 8.0 Hz, 1H), 7.88 (t, *J* = 4.0 Hz, 1H), 7.72-7.64 (m, 2H), 7.58 (t, *J* = 7.8 Hz, 1H). $^{13}C\{^1H\}$ NMR (126 MHz, $CDCl_3$, ppm): δ 185.6, 161.0, 147.9, 145.9, 134.9, 134.3, 134.0, 133.9, 131.8, 129.5, 129.4, 128.4, 126.9, 123.2. IR ($CHCl_3$): ν_{max} 3436, 2926, 1666, 1481, 1297, 1144 cm^{-1}. ESI-MS: *m/z* 251.08 $[M+H]^+$. HRMS (ESI-TOF) m/z: $[M+H]^+$ Calcd for $C_{15}H_{11}N_2O_2$ 251.0815; Found 251.0812.

*Quinazolin-4(3H)-one (**13**).*[29,42] Light pink solid. yield: 55% (59 mg). m.p. 218-220 °C. ^1H NMR (400 MHz, DMSO-d_6, ppm): δ 12.25 (s, 1H), 8.17-8.07 (m, 2H), 7.82 (t, *J* = 7.2 Hz, 1H), 7.67 (d, *J* = 8.1 Hz, 1H), 7.53 (t, *J* = 7.4 Hz, 1H). $^{13}C\{^1H\}$ NMR (101 MHz, DMSO-d_6, ppm): δ 162.1, 148.4, 145.1, 134.6, 127.1, 126.5, 125.9, 122.4. IR ($CHCl_3$): ν_{max} 3417, 2921, 1675, 1517, 1453, 1110 cm^{-1}. ESI-MS: *m/z* 147.04 $[M+H]^+$. HRMS (ESI-TOF) m/z: $[M+H]^+$ Calcd for $C_8H_7N_2O$ 147.0553; Found 147.0570.

NLRP3 Inflammasome Activation Assay. J774A.1 cells were seeded at a density of (0.4×10^6 cells/mL) in 24 well plates. Cells were primed with LPS (1 μg/mL) for 5.5 h in DMEM with 10 % FBS and then treated with different compounds or vehicle (DMSO) in serum free media for 1 h. Followed by incubation with test compounds or vehicle, the cells were stimulated with ATP (3 mM for 30 minutes). Supernatants were collected and analyzed for IL-1β levels by ELISA (Invitrogen, Ebiosciences). IL-1β levels in the supernatants were observed through IL-1β ELISA kit (Invitrogen, Ebioscience) according to manufacturer's instruction. The absorbance for the

cytokine was measured at 450 nm. The concentration of estimated cytokine was normalized with the total protein amount extracted using NaCl-Triton X lysis buffer.

Western-blot Analysis. Cell lysates were prepared in RIPA buffer (50 mM Tris-HCl [pH 7.5], 150 mM NaCl, 1 mM EDTA, 1 mM NaF, 1% Nonidet P-40, and, 0.25% Na-deoxycholate) with complete protease inhibitor cocktail (Sigma-Aldrich), 1 mM PMSF, 1 mM sodium ortho-vanadate. The protein concentrations were determined by Bradford protein assay (Bio-Rad). The cell supernatants were collected and concentrated by strata clear resin (Agilent). Proteins were separated by SDS-PAGE gel electrophoresis and then transferred to PVDF membrane. The PVDF membrane was blocked in TBST containing 5% skimmed milk for 2 h at room temperature and kept for overnight incubation with IL-1β primary antibody at 4 °C. After washing, incubation was done with secondary antibody at room temperature for 1-2 h and was then developed by using ECL (Millipore). The level of IL-1β released in the supernatants was measured through IL-1β ELISA kit (Invitrogen, Ebioscience) according to the manufacturer's instructions.

Statistical Analysis. Data from biological experiments were analyzed using GraphPad Prism (version 6). Student's *t* tests (ANOVA) were performed to compare the groups (statistical analysis.$^{*}p < 0.025$; .$^{**}p < 0.01$; .$^{***}p < 0.005$)

ACKNOWLEDGEMENTS. Authors thanks analytical department IIIM for analytical support. M. Abdullaha and M. Ali thanks UGC for research fellowship. S. Mohammed is thankful to CSIR for research fellowship. The financial support from CSIR YSA grant (P90807) is gratefully acknowledged.

AUTHOR INFORMATION.

Corresponding Author

*Tel: +91-191-2586333; Tel: +91-191-2585006 (Extn. 345). E-mail: sbharate@iiim.ac.in, sandipbharate@gmail.com (S.B.B.)

ORCID: 0000-0001-6081-5787

Notes

The authors declare no competing financial interest.

SUPPORTING INFORMATION AVAILABLE: NMR spectra scans and HRMS/ HPLC spectra scans for some compounds. This material is available free of charge *via* the Internet at http://pubs.acs.org.

REFERENCES

(1) (a) White, C. S.; Lawrence, C. B.; Brough, D.; Rivers-Auty, J. Inflammasomes as Therapeutic Targets for Alzheimer's disease. *Brain Pathol.* **2017**, *27*, 223-234; (b) Yin, J.; Zhao, F.; Chojnacki, J. E.; Fulp, J.; Klein, W. L.; Zhang, S.; Zhu, X. NLRP3 Inflammasome Inhibitor Ameliorates Amyloid Pathology in a Mouse Model of Alzheimer's Disease. *Mol. Neurobiol.* **2018**, *55*, 1977-1987; (c) Tan, M. S.; Yu, J. T.; Jiang, T.; Zhu, X. C.; Tan, L. The NLRP3 inflammasome in Alzheimer's disease. *Mol. Neurobiol.* **2013**, *48*, 875-882; (d) Ahmed, M. E.; Iyer, S.; Thangavel, R.; Kempuraj, D.; Selvakumar, G. P.; Raikwar, S. P.; Zaheer, S.; Zaheer, A. Co-Localization of Glia Maturation Factor with NLRP3 Inflammasome and Autophagosome Markers in Human Alzheimer's Disease Brain. *J. Alzheimers Dis.* **2017**, *60*, 1143-1160.

(2) (a) Zhai, Y.; Meng, X.; Luo, Y.; Wu, Y.; Ye, T.; Zhou, P.; Ding, S.; Wang, M.; Lu, S.; Zhu, L.; Sun, G.; Sun, X. Notoginsenoside R1 Ameliorates Diabetic Encephalopathy by Activating the Nrf2 Pathway and Inhibiting NLRP3 Inflammasome Activation. *Oncotarget* **2018**, *9*, 9344-9363; (b) Zhou, L.; Huang, W.; Xu, Y.; Gao, C.; Zhang, T.; Guo, M.; Liu, Y.; Ding, J.;

Qin, L.; Xu, Z.; Long, Y.; Xu, Y. Sweet Taste Receptors Mediated ROS-NLRP3 Inflammasome Signaling Activation: Implications for Diabetic Nephropathy. *J. Diabetes Res.* **2018**, *2018*, Article ID 7078214; (c) Zhai, Y.; Meng, X.; Ye, T.; Xie, W.; Sun, G.; Sun, X. Inhibiting the NLRP3 Inflammasome Activation with MCC950 Ameliorates Diabetic Encephalopathy in db/db Mice. *Molecules* **2018**, *23*, pii: E522.

(3) Zhao, C.; Gu, Y.; Zeng, X.; Wang, J. NLRP3 Inflammasome Regulates Th17 Differentiation in Rheumatoid Arthritis. *Clin. Immunol.* **2018**, *197*, 154-160.

(4) (a) Wu, X.; Dong, L.; Lin, X.; Li, J. Relevance of the NLRP3 Inflammasome in the Pathogenesis of Chronic Liver Disease. *Front. Immunol.* **2017**, *8*, 1728; (b) Ma, X.; Zheng, X.; Pan, L.; Zhang, X. NLRP3 Inflammasome Activation In Liver Cirrhotic Patients. *Biochem. Biophys. Res. Commun.* **2018**, *505*, 40-44.

(5) Yang, G.; Yeon, S. H.; Lee, H. E.; Kang, H. C.; Cho, Y. Y.; Lee, H. S.; Lee, J. Y. Suppression of NLRP3 Inflammasome by Oral Treatment with Sulforaphane Alleviates Acute Gouty Inflammation. *Rheumatology* **2018**, *57*, 727-736.

(6) (a) Yamaguchi, Y.; Kurita-Ochiai, T.; Kobayashi, R.; Suzuki, T.; Ando, T. Regulation of the NLRP3 Inflammasome in Porphyromonas Gingivalis-Accelerated Periodontal Disease. *Inflamm. Res.* **2017**, *66*, 59-65; (b) Yang, S. J.; Shao, G. F.; Chen, J. L.; Gong, J. The NLRP3 Inflammasome: An Important Driver of Neuroinflammation in Hemorrhagic Stroke. *Cell Mol. Neurobiol.* **2018**, *38*, 595-603; (c) Xiao, Y.; Xu, W.; Su, W. NLRP3 Inflammasome: A Likely Target for the Treatment of Allergic Diseases. *Clin. Exp. Allergy* **2018**, *48*, 1080-1091; (d) Wang, H.; Lv, C.; Wang, S.; Ying, H.; Weng, Y.; Yu, W. NLRP3 Inflammasome Involves in the Acute Exacerbation of Patients with Chronic Obstructive Pulmonary Disease. *Inflammation* **2018**, *41*, 1321-1333; (e) Toldo, S.; Abbate, A. The NLRP3 Inflammasome in Acute Myocardial

Infarction. *Nat. Rev. Cardiol.* **2018**, *15*, 203-214; (f) Perera, A. P.; Sajnani, K.; Dickinson, J.; Eri, R.; Korner, H. NLRP3 Inflammasome in Colitis and Colitis-Associated Colorectal Cancer. *Mamm. Genome* **2018**, 29, 817-830; (g) Moossavi, M.; Parsamanesh, N.; Bahrami, A.; Atkin, S. L.; Sahebkar, A. Role of the NLRP3 Inflammasome in Cancer. *Mol. Cancer* **2018**, *17*, 158; (h) Molyvdas, A.; Georgopoulou, U.; Lazaridis, N.; Hytiroglou, P.; Dimitriadis, A.; Foka, P.; Vassiliadis, T.; Loli, G.; Phillipidis, A.; Zebekakis, P.; Germenis, A. E.; Speletas, M.; Germanidis, G. The Role of the NLRP3 Inflammasome and the Activation of IL-1beta in the Pathogenesis of Chronic Viral Hepatic Inflammation. *Cytokine* **2018**, *110*, 389-396; (i) Mangan, M. S. J.; Olhava, E. J.; Roush, W. R.; Seidel, H. M.; Glick, G. D.; Latz, E. Targeting The NLRP3 Inflammasome In Inflammatory Diseases. *Nat. Rev. Drug Discov.* **2018**, *17*, 588-606; (j) Wu, S.; Huang, J. Resveratrol Alleviates *Staphylococcus aureus* Pneumonia by Inhibition of the NLRP3 Inflammasome. *Exp. Ther. Med.* **2017**, *14*, 6099-6104.

(7) Lu, W. L.; Song, D. Z.; Yue, J. L.; Wang, T. T.; Zhou, X. D.; Zhang, P.; Zhang, L.; Huang, D. M. NLRP3 Inflammasome May Regulate Inflammatory Response of Human Periodontal Ligament Fibroblasts in an Apoptosis-Associated Speck-Like Protein Containing a Card (Asc)-Dependent Manner. *Int. Endod. J.* **2017**, *50*, 967-975.

(8) (a) Baldwin, A. G.; Brough, D.; Freeman, S. Inhibiting the Inflammasome: A Chemical Perspective. *J. Med. Chem.* **2016**, *59*, 1691-1710; (b) Shao, B. Z.; Xu, Z. Q.; Han, B. Z.; Su, D. F.; Liu, C. NLRP3 Inflammasome and its Inhibitors: A Review. *Front. Pharmacol.* **2015**, *6*, 262.

(9) Lamkanfi, M.; Mueller, J. L.; Vitari, A. C.; Misaghi, S.; Fedorova, A.; Deshayes, K.; Lee, W. P.; Hoffman, H. M.; Dixit, V. M. Glyburide Inhibits the Cryopyrin/Nalp3 Inflammasome. *J. Cell Biol.* **2009**, *187*, 61-70.

(10) Juliana, C.; Fernandes-Alnemri, T.; Wu, J.; Datta, P.; Solorzano, L.; Yu, J. W.; Meng, R.; Quong, A. A.; Latz, E.; Scott, C. P.; Alnemri, E. S. Anti-Inflammatory Compounds Parthenolide and Bay 11-7082 are Direct Inhibitors of the Inflammasome. *J. Biol. Chem.* **2010**, *285*, 9792-9802.

(11) Cocco, M.; Miglio, G.; Giorgis, M.; Garella, D.; Marini, E.; Costale, A.; Regazzoni, L.; Vistoli, G.; Orioli, M.; Massulaha-Ahmed, R.; Detraz-Durieux, I.; Groslambert, M.; Py, B. F.; Bertinaria, M. Design, Synthesis, and Evaluation of Acrylamide Derivatives as Direct NLRP3 Inflammasome Inhibitors. *ChemMedChem* **2016**, *11*, 1790-1803.

(12) (a) Coll, R. C.; Robertson, A. A.; Chae, J. J.; Higgins, S. C.; Munoz-Planillo, R.; Inserra, M. C.; Vetter, I.; Dungan, L. S.; Monks, B. G.; Stutz, A.; Croker, D. E.; Butler, M. S.; Haneklaus, M.; Sutton, C. E.; Nunez, G.; Latz, E.; Kastner, D. L.; Mills, K. H.; Masters, S. L.; Schroder, K.; Cooper, M. A.; O'Neill, L. A. A Small-Molecule Inhibitor of the NLRP3 Inflammasome for the Treatment of Inflammatory Diseases. *Nat. Med.* **2015**, *21*, 248-255; (b) Perera, A. P.; Fernando, R.; Shinde, T.; Gundamaraju, R.; Southam, B.; Sohal, S. S.; Robertson, A. A. B.; Schroder, K.; Kunde, D.; Eri, R. MCC950, A Specific Small Molecule Inhibitor of NLRP3 Inflammasome Attenuates Colonic Inflammation In Spontaneous Colitis Mice. *Sci. Rep.* **2018**, *8*, 8618.

(13) Keystone, E. C.; Wang, M. M.; Layton, M.; Hollis, S.; McInnes, I. B. Clinical Evaluation of the Efficacy of the P2X7 Purinergic Receptor Antagonist AZD9056 on the Signs And Symptoms of Rheumatoid Arthritis in Patients with Active Disease Despite Treatment with Methotrexate or Sulphasalazine. *Ann. Rheum. Dis.* **2012**, *71*, 1630-1635.

(14) (a) Shi, J.; Zhao, W.; Ying, H.; Zhang, Y.; Du, J.; Chen, S.; Li, J.; Shen, B. Estradiol Inhibits NLRP3 Inflammasome in Fibroblast-Like Synoviocytes Activated by

Lipopolysaccharide and Adenosine Triphosphate. *Int. J. Rheum. Dis.* **2018**, *21*, 2002-2010; (b) Thakkar, R.; Wang, R.; Sareddy, G.; Wang, J.; Thiruvaiyaru, D.; Vadlamudi, R.; Zhang, Q.; Brann, D. NLRP3 Inflammasome Activation in the Brain after Global Cerebral Ischemia and Regulation by 17beta-Estradiol. *Oxid. Med. Cell Longev.* **2016**, *2016*, 8309031.

(15) (a) Nanda, A. K.; Ganguli, S.; Chakraborty, R. Antibacterial Activity of Some 3-(Arylideneamino)-2-phenylquinazoline-4(3H)-ones: Synthesis and Preliminary QSAR Studies. *Molecules* **2007**, *12*, 2413-2426; (b) Kikuchi, H.; Yamamoto, K.; Horoiwa, S.; Hirai, S.; Kasahara, R.; Hariguchi, N.; Matsumoto, M.; Oshima, Y. Exploration of a New Type of Antimalarial Compounds Based on Febrifugine. *J. Med. Chem.* **2006**, *49*, 4698-4706; (c) Chan, J. H.; Hong, J. S.; Kuyper, L. F.; Baccanari, D. P.; Joyner, S. S.; Tansik, R. L.; Boytos, C. M.; Rudolph, S. K. Selective Inhibitors of *Candida albicans* Dihydrofolate Reductase: Activity and Selectivity of 5-(Arylthio)-2,4-Diaminoquinazolines. *J. Med. Chem.* **1995**, *38*, 3608-3616; (d) Yen, M. H.; Sheu, J. R.; Peng, I. H.; Lee, Y. M.; Chern, J. W. Pharmacological Activity of DC-015, a Novel Potent and Selective Alpha 1-Adrenoceptor Antagonist. *J. Pharm. Pharmacol.* **1996**, *48*, 90-95; (e) Chandrika, P. M.; Yakaiah, T.; Rao, A. R. R.; Narsaiah, B.; Reddy, N. C.; Sridhar, V.; Rao, J. V. Synthesis of Novel 4,6-Disubstituted Quinazoline Derivatives, Their Anti-Inflammatory and Anti-Cancer Activity (Cytotoxic) Against U937 Leukemia Cell Lines. *Eur. J. Med. Chem.* **2008**, *43*, 846-852; (f) Dupuy, M.; Pinguet, F.; Chavignon, O.; Chezal, J. M.; Teulade, J. C.; Chapat, J. P.; Blache, Y. Synthesis and In Vitro Cytotoxic Evaluation of New Derivatives of Pyrido[1,2-A]Benzimidazolic Ring System: The Pyrido[1',2':1,2]Imidazo[4,5-H]Quinazolines. *Chem. Pharm. Bull.* **2001**, *49*, 1061-1065; (g) Takase, Y.; Saeki, T.; Watanabe, N.; Adachi, H.; Souda, S.; Saito, I. Cyclic GMP Phosphodiesterase Inhibitors. 2. Requirement of 6-Substitution of Quinazoline Derivatives for Potent and Selective Inhibitory Activity. *J. Med. Chem.* **1994**, *37*, 2106-2111; (h) Baba, A.; Kawamura, N.; Makino, H.; Ohta, Y.; Taketomi, S.;

Sohda, T. Studies on Disease-Modifying Antirheumatic Drugs: Synthesis of Novel Quinoline and Quinazoline Derivatives and Their Anti-Inflammatory Effect. *J. Med. Chem.* **1996**, *39*, 5176-5182; (i) Yarosh, D. B.; Galvin, J. W.; Nay, S. L.; Pena, A. V.; Canning, M. T.; Brown, D. A. Anti-Inflammatory Activity in Skin by Biomimetic of *Evodia rutaecarpa* Extract from Traditional Chinese Medicine. *J. Dermatol. Sci.* **2006**, *42*, 13-21; (j) Archana; Shrivastava, V. K.; Chandra, R.; Kumar, A. Synthesis of Potential Quinazolinonyl Pyrazolines and Quinazolinyl Isoxazolines as Anticonvulsant Agents. *Indian J. Chem* **2002**, *41B*, 2371-2375; (k) Daidone, G.; Maggio, B.; Raffa, D.; Plescia, S.; Bajardi, M. L.; Caruso, A.; Cutuli, V. M. C.; Amico-Roxas, M. Synthesis and Pharmacological Study of Ethyl 1-Methyl-5-[2-Substituted-4-Oxo-3(4h)-Quinazolinyl]-1H-Pyrazole-4-Acetates. *Eur. J. Med. Chem.* **1994**, *29*, 707-711.

(16) (a) He, L.; Li, H.; Chen, J.; Wu, X.-F. Recent Advances In 4(*3H*)-Quinazolinone Syntheses. *RSC Adv.* **2014**, *4*, 12065-12077; (b) Connolly, D. J.; Cusack, D.; O'Sullivan, T. P.; Guiry, P. J. Synthesis of Quinazolinones and Quinazolines. *Tetrahedron* **2005**, *61*, 10153-10202; (c) Mhaske, S. B.; Argade, N. P. The Chemistry of Recently Isolated Naturally Occurring Quinazolinone Alkaloids. *Tetrahedron* **2006**, *62*, 9787-9826.

(17) Abdel-Jalil, R. J.; Aldoqum, H. M.; Ayoub, M. T.; Voelter, W. Synthesis And Antitumor Activity of 2-Aryl-7-Fluoro-6-(4-Methyl-1-Piperazinyl)-4(3H)-Quinazolinones. *Heterocycles* **2005**, *65*, 2061.

(18) Mitobe, Y.; Ito, S.; Mizutani, T.; Nagase, T.; Sato, N.; Tokita, S. Development of a Selective and Potent Radioactive Ligand for Histamine H(3) Receptors: A Compound Potentially Useful for Receptor Occupancy Studies. *Bioorg. Med. Chem. Lett.* **2009**, *19*, 4075-4078.

(19) Balakumar, C.; Lamba, P.; Kishore, D. P.; Narayana, B. L.; Rao, K. V.; Rajwinder, K.; Rao, A. R.; Shireesha, B.; Narsaiah, B. Synthesis, Anti-Inflammatory Evaluation and

Docking Studies of Some New Fluorinated Fused Quinazolines. *Eur. J. Med. Chem.* **2010**, *45*, 4904-4913.

(20) Hisano, T.; Ichikawa, M.; Nakagawa, A.; Tsuji, M. Studies on Organosulfur Compounds. Xii. Syntheses and Pharmacological Activities of 2-Heterocyclic Substituted 4(*3H*)-Quinazolinones. *Chem. Pharm. Bull.* **1975**, *23*, 1910-1916.

(21) Wei, H.; Li, T.; Zhou, Y.; Zhou, L.; Zeng, Q. Copper-Catalyzed Domino Synthesis of Quinazolin-4(*3H*)-ones from (Hetero)arylmethyl Halides, Bromoacetate, and Cinnamyl Bromide. *Synthesis* **2013**, *45*, 3349-3354.

(22) (a) Hikawa, H.; Ino, Y.; Suzuki, H.; Yokoyama, Y. Pd-Catalyzed Benzylic C-H Amidation with Benzyl Alcohols in Water: A Strategy to Construct Quinazolinones. *J. Org. Chem.* **2012**, *77*, 7046-7051; (b) Zhou, J.; Fang, J. One-Pot Synthesis of Quinazolinones via Iridium-Catalyzed Hydrogen Transfers. *J. Org. Chem.* **2011**, *76*, 7730-7736; (c) Sharif, M.; Opalach, J.; Langer, P.; Beller, M.; Wu, X.-F. Oxidative Synthesis of Quinazolinones and Benzothiadiazine 1,1-Dioxides from 2-Aminobenzamide and 2-Aminobenzenesulfonamide with Benzyl Alcohols and Aldehydes. *RSC Adv.* **2014**, *4*, 8–17; (d) Ge, W.; Zhu, X.; Wei, Y. Iodine-Catalyzed Oxidative System for Cyclization of Primary Alcohols with *O*-Aminobenzamides to Quinazolinones Using DMSO as the Oxidant in Dimethyl Carbonate. *RSC Adv.* **2013**, *3*, 10817-10822.

(23) Nguyen, T. B.; Ermolenko, L.; Al-Mourabit, A. Selective Autoxidation of Benzylamines: Application to the Synthesis of Some Nitrogen Heterocycles. *Green Chem.* **2013**, *15*, 2713-2717.

(24) Wu, X.-F.; He, L.; Neumann, H.; Beller, M. Palladium-Catalyzed Carbonylative Synthesis of Quinazolinones from 2-Aminobenzamide and Aryl Bromides. *Chem. Eur. J.* **2013**, *19*, 12635-12638.

(25) Jiang, X.; Tang, T.; Wang, J.-M.; Chen, Z.; Zhu, Y.-M.; Ji, S.-J. Palladium-Catalyzed One-Pot Synthesis of Quinazolinones via tert-Butyl Isocyanide Insertion. *J. Org. Chem.* **2014**, *79*, 5082-5087.

(26) Purandare, A. V.; Gao, A.; Wan, H.; Somerville, J.; Burke, C.; Seachord, C.; Vaccaro, W.; Wityak, J.; Poss, M. A. Identification of Chemokine Receptor CCR4 Antagonist. *Bioorg. Med. Chem. Lett.* **2005**, *15*, 2669-2672.

(27) Potewar., T. M.; Nadaf., R. N.; Daniel., T.; Lahoti, R. J.; Srinivasan, K. V. A Novel One-Pot Synthesis of 2-Aryl-4(3H)-Quinazolinones Using Room Temperature Ionic Liquid as Reaction Medium as well as Promoter. *Synth. Commun.* **2005**, *35*, 231-241.

(28) (a) Zhao, D.; Wang, T.; Li, J. X. Metal-Free Oxidative Synthesis of Quinazolinones Via Dual Amination of Sp3 C-H Bonds. *Chem. Commun.* **2014**, *50*, 6471-6474; (b) Li, Q.; Huang, Y.; Chen, T.; Zhou, Y.; Xu, Q.; Yin, S.-F.; Han, L.-B. Copper-Catalyzed Aerobic Oxidative Amination of sp3C–H Bonds: Efficient Synthesis of 2-Hetarylquinazolin-4(3H)-ones. *Org. Lett.* **2014**, *16*, 3672-3675.

(29) Yang, X.; Cheng, G.; Shen, J.; Kuai, C.; Cui, X. Cleavage Of The C–C Triple Bond of Ketoalkynes: Synthesis of 4(*3H*)-Quinazolinones. *Org. Chem. Front.* **2015**, *2*, 366–368.

(30) (a) Mohammed, S.; Vishwakarma, R. A.; Bharate, S. B. Metal-free DBU Promoted Regioselective Synthesis of Isoxazoles and Isoxazolines. *RSC Adv.* **2015**, *5*, 3470-3473; (b) Mohammed, S.; Vishwakarma, R. A.; Bharate, S. B. Iodine Catalyzed Oxidative Synthesis of Quinazolin-4(3H)-ones and Pyrazolo[4,3-d]pyrimidin-7(6H)-ones via Amination of sp(3) C-H

Bond. *J. Org. Chem.* **2015**, *80*, 6915-6921; (c) Bharate, J. B.; Abbat, S.; Bharatam, P. V.; Vishwakarma, R. A.; Bharate, S. B. CuBr Catalyzed Aerobic Oxidative Coupling of 2-Aminopyridines with Cinnamaldehydes: Direct Access to 3-Formyl-2-Phenyl-Imidazo[1,2-A]Pyridines. *Org. Biomol. Chem.* **2015**, *13*, 7790-7794; (d) Bharate, J. B.; Bharate, S. B.; Vishwakarma, R. A. Metal-Free, Ionic Liquid-Mediated Synthesis of Functionalized Quinolines. *ACS Comb. Sci.* **2014**, *16*, 624–630; (e) Bharate, J. B.; Guru, S. K.; Jain, S. K.; Meena, S.; Singh, P. P.; Bhushan, S.; Singh, B.; Bharate, S. B.; Vishwakarma, R. A. Cu-Mn Spinel Oxide Catalyzed Synthesis of Imidazo[1,2-a]pyridines Through Domino Three-Component Coupling And 5-Exo-Dig Cyclization in Water. *RSC Adv.* **2013**, *3*, 20869–20876; (f) Bharate, J. B.; Wani, A.; Sharma, S.; Reja, S. I.; Kumar, M.; Vishwakarma, R. A.; Kumar, A.; Bharate, S. B. Synthesis, Antioxidant, Neuroprotective and P-Glycoprotein Induction Activity of 4-Arylquinoline-2-Carboxylates. *Org. Biomol. Chem.* **2014**, *12*, 6267-6277; (g) Bharate, S. B.; Mudududdla, R.; Bharate, J. B.; Battini, N.; Battula, S.; Yadav, R. R.; Singh, B.; Vishwakarma, R. A. Tandem One-Pot Synthesis of Flavans by Recyclable Silica-$HClO_4$ Catalyzed Knoevenagel Condensation and [4+2]-Diels-Alder Cycloaddition. *Org. Biomol. Chem.* **2012**, *10*, 5143-5150; (h) Bharate, J. B.; Sharma, R.; Singh, B.; Aravinda, S.; Gupta, V. K.; Bharate, S. B.; Vishwakarma, R. A. Montmorillonite Clay Catalyzed Synthesis of Functionalized Pyrroles Through Domino Four-Component Coupling of Amines, Aldehydes, 1,3-Dicarbonyl Compounds And Nitroalkanes. *RSC Adv.* **2013**, *3*, 21736–21742; (i) Bharate, S. B.; Padala, A.; Dar, B. A.; Yadav, R. R.; Singh, B.; Vishwakarma, R. A. Montmorillonite Clay Cu(II)Catalyzed Domino One-Pot Multicomponent Synthesis of 3,5-Disubstituted Isoxazoles. *Tetrahedron Lett.* **2013**, *54*, 3558-3561.

(31) Hu, Z.; Yan, C.; Liu, P.; Huang, Z.; Ma, R.; Zhang, C.; Wang, R.; Zhang, Y.; Martinon, F.; Miao, D.; Deng, H.; Wang, J.; Chang, J.; Chai, J. Crystal Structure of NLRC4 Reveals Its Autoinhibition Mechanism. *Science* **2013**, *341*, 172-175.

(32) Yang, J.; Yan, R.; Roy, A.; Xu, D.; Poisson, J.; Zhang, Y. The I-TASSER Suite: Protein Structure And Function Prediction. *Nat. Methods* **2015**, *12*, 7-8.

(33) Deligeorgiev, T. G.; Kaloyanova, S.; Vasilev, A.; Vaquero, J. J.; Alvarez-Builla, J.; Cuadro, A. M. Novel Environmentally Benign Procedure for the Synthesis of 2-Aryl- and 2-Hetaryl-4(*3H*)-Quinazolinones. *Color. Technol.* **2010**, *126*, 24-30.

(34) (a) Lee, W.; Ortwine, D. F.; Bergeron, P.; Lau, K.; Lin, L.; Malek, S.; Nonomiya, J.; Pei, Z.; Robarge, K. D.; Schmidt, S.; Sideris, S.; Lyssikatos, J. P. A Hit To Lead Discovery of Novel N-Methylated Imidazolo-, Pyrrolo-, and Pyrazolo-Pyrimidines as Potent and Selective Mtor Inhibitors. *Bioorg. Med. Chem. Lett.* **2013**, *23*, 5097-5104; (b) Terrett, N. K.; Bell, A. S.; Brown, D.; Ellis, P. Sildenafil (VIAGRATM), a Potent And Selective Inhibitor of Type 5 CGMP Phosphodiesterase with Utility for the Treatment of Male Erectile Dysfunction. *Bioorg. Med. Chem. Lett.* **1996**, *6*, 1819-1824.

(35) Zhu, Y. P.; Jia, F. C.; Liu, M. C.; Wu, A. X. A Multipathway Coupled Domino Strategy: Metal-Free Oxidative Cyclization for One-Pot Synthesis of 2-Acylbenzothiazoles from Multiform Substrates. *Org. Lett.* **2012**, *14*, 4414-4417.

(36) Chen, D. F.; Han, Z. Y.; He, Y. P.; Yu, J.; Gong, L. Z. Metal-Free Oxidation/C(SP3)-H Functionalization of Unactivated Alkynes Using Pyridine-N-Oxide as the External Oxidant. *Angew. Chem. Int. Ed.* **2012**, *51*, 12307.

(37) (a) Zhu, Y. P.; Jia, F. C.; Liu, M. C.; Wu, L. M.; Cai, Q.; Gao, Y.; Wu, A. X. I_2-CF_3SO_3H Synergistic Promoted SP3 C-H Bond Diarylation of Aromatic Ketones. *Org. Lett.*

2012, *14*, 5378-5381; (b) Wu, X.; Gao, Q.; Liu, S.; Wu, A. I_2-Catalyzed Oxidative Cross-Coupling of Methyl Ketones and Benzamidines Hydrochloride: A Facile Access to α-Ketoimides. *Org. Lett.* **2014**, *16*, 2888-2891.

(38) Nobuta, T.; Hirashima, S.; Tada, N.; Miura, T.; Itoh, A. One-Pot Metal-Free Syntheses of Acetophenones from Styrenes Through Aerobic Photo-Oxidation and Deiodination with Iodine. *Org. Lett.* **2011**, *13*, 2576-2579.

(39) Xu, W.; Jin, Y.; Liu, H.; Jiang, Y.; Fu, H. Copper-Catalyzed Domino Synthesis of Quinazolinones via Ullmann-Type Coupling and Aerobic Oxidative C−H Amidation. *Org. Lett.* **2011**, *13*, 1274–1277.

(40) Hu, B. Q.; Wang, L. X.; Yang, L.; Xiang, J. F.; Tang, Y. L. Copper-Catalyzed Intramolecular C–C Bond Cleavage to Construct 2-Substituted Quinazolinones. *Eur. J. Org. Chem.* **2015**, *2015*, 4504-4509.

(41) Zhang, J.; Ren, D.; Ma, Y.; Wang, W.; Wu, H. Cuo Nanoparticles Catalyzed Simple and Efficient Synthesis of 2,3-Dihydroquinazolin-4(*1H*)-Ones and Quinazolin-4(*3H*)-Ones Under Ultrasound Irradiation in Aqueous Ethanol Under Ultrasound Irradiation in Aqueous Ethanol. *Tetrahedron* **2014**, *70*, 5274-5282.

(42) Kim, N. Y.; Cheon, C. H. Synthesis of Quinazolinones From Anthranilamides and Aldehydes Via Metal-Free Aerobic Oxidation in DMSO. *Tetrahedron Lett.* **2014**, *55*, 2340-2344.

(43) Sharma, R.; Vishwakarma, R. A.; Bharate, S. B. Bimetallic Cu-Mn-Catalyzed Synthesis of 2-Arylquinazolin-4(3H)-ones: Aqueous Ammonia as Source of a Ring Nitrogen Atom. *Eur. J. Org. Chem.* **2016**, *2016*, 5227-5233.

(44) Tian, X.; Song, L.; Li, E.; Wang, Q.; Yu, W.; Chang, J. Metal-Free One-Pot Synthesis of 1,3-Diazaheterocyclic Compounds Via I_2-Mediated Oxidative C–N Bond Formation. *RSC Adv.* **2015**, *5*, 62194-62201.

(45) Zhu, Y. P.; Fei, Z.; Liu, M. C.; Jia, F. C.; Wu, A. X. Direct One-Pot Synthesis Of Luotonin F And Analogues Via Rational Logical Design. *Org. Lett.* **2013**, *15*, 378-381.